MS. CAROLIN DAHMS (Orcid ID : 0000-0002-3283-7820)

PROF. JUHA MERILÄ (Orcid ID : 0000-0001-9614-0072)

Article type : Original Article

Cast Away in the Adriatic: Low Degree of Parallel Genetic Differentiation in Three-Spined Sticklebacks

Short title: Parallel evolution under low gene flow

Carolin Dahms[1], Petri Kemppainen[1], Linda N. Zanella[2], Davor Zanella[2], Antonella Carosi[3], Juha Merilä[1,4], Paolo Momigliano[1]

[1]*Ecological Genetics Research Unit, Organismal and Evolutionary Biology Research Programme, Faculty of Biological and Environmental Sciences, FI-00014 University of Helsinki, Finland*

[2]*Department of Zoology, Faculty of Science, University of Zagreb, Rooseveltov trg 6, 10000 Zagreb, Croatia*

[3]*Department of Chemistry, Biology and Biotechnologies, University of Perugia, via Elce di Sotto 8, 06123 Perugia, Italy*

[4] *Division for Ecology and Biodiversity, School of Biological Sciences, Faculty of Science, The University of Hong Kong, Hong Kong SAR*

Correspondence to: carolin.dahms.ac@gmail.com, paolo.momigliano@gmail.com

ABSTRACT

The three-spined stickleback (*Gasterosteus aculeatus*) has repeatedly and independently adapted to freshwater habitats from standing genetic variation (SGV) following colonisation from the sea. However, in the Mediterranean Sea *G. aculeatus* is believed to have gone extinct, thus the spread of locally adapted alleles between different freshwater populations via the sea since then has been highly unlikely. This is expected to limit parallel evolution, i.e., the extent to which phylogenetically related alleles can be shared among independently colonised freshwater populations. Using whole genome and 2b-RAD sequencing data, we compared levels of genetic differentiation and genetic parallelism of 15 Adriatic stickleback populations to 19 Pacific, Atlantic and Caspian populations, where gene flow between freshwater populations across extant marine populations is still possible. Our findings support previous studies suggesting that Adriatic populations are highly differentiated (average $F_{ST} \approx 0.45$), of low genetic diversity and connectivity, and likely to stem from multiple independent colonisations during the Pleistocene. Linkage disequilibrium network analyses in combination with linear mixed models nevertheless

revealed several parallel marine-freshwater differentiated genomic regions, although still not to the extent observed elsewhere in the world. We hypothesize that current levels of genetic parallelism in the Adriatic lineages are a relic of freshwater adaptation from SGV prior to the extinction of marine sticklebacks in the Mediterranean that has persisted despite substantial genetic drift experienced by the Adriatic stickleback isolates.

Keywords: *Gasterosteus aculeatus*, gene flow, parallel evolution, adaptation, three-spine stickleback

INTRODUCTION

Allele frequency changes caused by adaptive evolution have extensively shaped patterns of genetic variation and adaptive radiations in the wild (Hughes, 1999; Leinonen et al., 2013; Mayr, 1963; Merilä & Crnokrak, 2001). Considering the increasing rate of environmental change, understanding the factors that underlie and determine the adaptive potential of species is more relevant than ever (Gienapp et al., 2008; Parmesan, 2006; Razgour et al., 2019). The rate and degree at which populations are expected to respond to natural selection is thought to depend significantly on demographic and genetic characteristics of populations and the traits under selection (Lynch & Walsh, 1998). For instance, small populations are less likely to carry potentially adaptive alleles and are more likely to be subject to strong genetic drift depleting genetic variation and reducing the effect of selection than large populations, and thus, are likely subject to reduced adaptive potential (Lanfear et al., 2014; Stern & Orgogozo, 2009, Willi et al., 2006). Constraints on local adaptation may also be imposed by the genetic architecture of the traits under selection (Arnold, 1992; Kemppainen et al., 2021), or strong gene flow; the latter possibly resulting in gene swamping when maladaptive alleles of immigrant individuals replace locally adapted alleles (Lenormand, 2002).

Although traditional population genetic theory posits that gene flow constrains the likelihood of populations adapting to local conditions (Gomulkiewicz et al., 1999; Mayr, 1963), growing evidence has shown that under certain circumstances gene flow and admixture may facilitate local adaptation by increasing the effective population size (N_e) of populations and by supplying novel genetic variation to support local adaptation (Kirkpatrick & Peischl, 2013; Marques et al., 2019; Tigano & Friesen, 2016). The three-spined stickleback *Gasterosteus aculeatus*, a well-studied model organism in population genetics, illustrates the importance of gene flow in local adaptation, where the same standing genetic variation (SGV) segregating at low frequencies in the sea is repeatedly fuelling local adaptation in independently derived freshwater populations. In turn, this SGV is constantly being replenished by recurrent gene flow from different freshwater populations (the 'transporter hypothesis', Schluter and Conte, 2009). This scenario of gene flow between marine and freshwater populations is also the underlying cause of why three-spined stickleback populations frequently exhibit high levels of genetic parallelism in response to freshwater colonization (Barrett & Schluter, 2008; Schluter & Conte, 2009). However, among global *G. aculeatus* populations the degree of parallel genetic changes that result in similar phenotypes through shared molecular evolutionary pathways (Arendt & Reznick, 2008) might not be as high or as geographically uniform as previously assumed (Fang et al., 2021; Ferchaud & Hansen, 2016; Liu et al., 2018; Terekhanova et al., 2014). The explanation for this appears to be varying levels and access to SGV for freshwater adaptation in different parts of the world (Fang et al., 2020a; Fang et al., 2021, Kemppainen et al., 2021). Pools of SGV are significantly influenced by the ancestral (marine) populations' N_e, which is the single most important determinant of genetic drift in a population (MacPherson & Nuismer, 2017; Thompson et al., 2019), as well as by population connectivity which enables access to the same freshwater-adapted alleles across wider geographic areas (Bailey et al., 2017; Lee & Coop, 2017; Ralph & Coop, 2015; Terekhanova et al., 2014). In the same vein, past demographic events – in particular range expansions, during which genetic diversity is lost due to bottlenecks and founder effects (Barton & Charlesworth, 1984; Fang et al., 2020a) – are key to understanding geographic heterogeneity in SGV in the sea.

Consistent with the historical colonization patterns of three spined sticklebacks, the levels of genetic parallelism in this species are highest in the ancestral Eastern Pacific region, where the species' presence dates back to around 17 Mya (million years ago; Betancur et al., 2015; Guo et al., 2019; Matschiner et al., 2011), and much lower in the younger Western Pacific populations (Fang et al., 2020a). Genetic parallelism is further reduced in the Atlantic Ocean which was recolonised around 36.9–346.5 kya (thousand years ago; Fang et al., 2018; Fang et al., 2020b). From the Atlantic, the three-spined stickleback rapidly colonized most of Europe, only to be eradicated from higher latitudes during the last glaciation (Fang et al., 2018; Schmitt, 2007). Remaining mostly unaffected by glaciations, southern European regions such as the Adriatic Sea basin provided refugia to retreating fauna (Schmitt, 2007), and later supplied migrants recolonizing northern Europe during the Last Interglacial period around 11.3–95.2 kya (DeFaveri et al., 2012; Fang et al., 2020b; Mäkinen & Merilä, 2008). However, most studies investigating the genetics and evolutionary history of three-spined sticklebacks have been conducted in the Pacific and Atlantic Oceans, whereas current knowledge on Mediterranean lineages is based on only a few studies using a limited number of genetic markers of genomic fragments (Araguas et al., 2012; Cano et al., 2008; DeFaveri et al., 2012; Lucek & Seehausen, 2015; Sanz et al., 2015) or sampling of a limited number of populations (Fang et al., 2020b; Fang et al., 2018).

While most freshwater populations globally have been derived post-glacially, the Adriatic three-spined stickleback lineage is thought to have its origin dating back to the Pleistocene, and thus harbours much of the ancestral diversity (Cano et al., 2008; DeFaveri et al., 2012; Mäkinen & Merilä, 2008; Sanz et al., 2015; Zanella et al., 2015). Indeed, Adriatic *G. aculeatus* populations are genetically and morphologically highly divergent from other European populations (Mäkinen et al., 2006; Mäkinen & Merilä, 2008; Zanella et al., 2009), which has prompted a proposal to assign them special conservation status (Cano et al., 2008). In contrast to European freshwater populations that range from the Mediterranean to Barents Sea, marine *G. aculeatus* populations are thought to be absent from the Mediterranean Sea (Lucek & Seehausen, 2015; Mäkinen et al., 2006), with only few low-plated populations confirmed in brackish lagoons along the French coast (Crivelli & Britton, 1987), and informal reports of individual sightings in Italian, Greek and Croatian lagoons (personal communication, L.N. Zanella). The extinction of the marine

population in the Mediterranean Sea has cut the access to the ancestral pool of SGV, and thus, there has likely been limited gene flow between Adriatic freshwater populations in recent history. Given their ancient origin and long period of isolation (Cano et al., 2008; DeFaveri et al., 2012; Fang et al., 2020a; Mäkinen & Merilä, 2008), the Adriatic Sea populations provide an interesting opportunity to test the extent to which the patterns of genetic parallelism seen elsewhere in the world depend on gene flow between freshwater and marine populations.

The aim of this study was to test the hypothesis that the levels of genetic parallelism in freshwater populations of three-spined sticklebacks in the Adriatic region are lower than anywhere else in the world. This could be expected for two distinct reasons. First, assuming that continued gene flow between marine and freshwater habitats is important in suppling genetic material for maintaining parallelism in freshwater adaptation, the long isolation of Adriatic populations might have reduced the degree of genetic parallelism (Kirkpatrick & Peischl, 2013; Ralph & Coop, 2015; Tigano & Friesen, 2016). Second, even if the separate Adriatic basin populations adapted to freshwater environments in parallel fashion at the time of the first invasion, their long isolation combined with genetic drift due to population size bottlenecks and low long-term N_e might have eroded genetic parallelism. To detect genomic regions involved in parallel evolution associated with marine-freshwater differentiation in the Adriatic Sea and elsewhere in the world, we used linkage disequilibrium network analyses (Kemppainen et al., 2015; Li et al., 2018) together with linear mixed models (Fang et al. 2021). In addition, given that population history is an important determinant of the likelihood of parallel evolution (Conte et al., 2012), we reconstructed demographic histories of the Adriatic three-spined stickleback populations to determine their divergence times, population size changes and connectivity. While we expect overall high differentiation and small N_e of Adriatic populations, we predict heterogeneity in demographic history and divergence, as suggested by previous studies (Mäkinen et al., 2006; Mäkinen & Merilä, 2008; Zanella et al., 2009).

MATERIALS AND METHODS

Study populations and sampling

This work follows from previous studies on the Adriatic region, which were now expanded to include the western Adriatic coast (Italy), look deeper into the southern Adriatic populations (Albania) and investigate the adjacent Ionian and Aegean populations (Greece). While one central Italian population (ICL) originates from the Tyrrhenian basin (western coast of central Italy) representing a pure Mediterranean outlier, all the aforementioned Southern European samples are collectively referred to as 'Adriatic' further on. A total of 258 samples representing both freshwater and marine ecotypes were included in this study. The samples covered a wide geographic range, encompassing the Eastern and Western Pacific, the Western Atlantic, Northern and Southern Europe, and the Caspian Sea (Figure 1, Supplementary Table S1). To investigate global patterns of parallelism, locations were grouped into five geographic regions – Eastern Pacific, Western Pacific, Trans-Atlantic, Caspian and Adriatic Sea (Figure 1). 174 samples from 15 locations (rivers, springs and ponds) in the Adriatic Sea region, one marine Caspian Sea location and two marine North Sea locations (SYL and TEX) were sequenced specifically for this study. Fish were caught with seine nets, minnow traps or by electrofishing, euthanized with an overdose of MS-222 and preserved in ethanol. Whole genome sequences of the remaining 84 individuals were retrieved from published studies (Feulner et al., 2015; Jones et al., 2012; Liu et al., 2016; Shanfelter et al., 2019; Vines et al., 2016; Yoshida et al., 2014; Yoshida et al., 2016) through the National Center for Biotechnology Information (NCBI). Four individuals of *Gasterosteus nipponicus*, a sister species of *G. aculeatus* thought to have diverged from the latter around 0.68 Mya (Kitano et al., 2009; Ravinet et al., 2018), were included as an outgroup in phylogenetic analyses. Information on coordinates, ecotype and population information on the sampled individuals and re-acquired samples is given in Supplementary Table S1.

DNA extraction, library preparation and sequencing

We carried out genome-wide genotyping using a streamlined restriction site–associated DNA (RAD) sequencing technique known as 2b-RAD (Wang et al., 2012). 2b-RAD libraries were built as detailed in Momigliano et al. (2018). Briefly, DNA was extracted using a DNeasy Blood and Tissue Kit (Qiagen) and a modified salting out protocol. For each sample, approximately 200 ng of DNA was digested with type II b enzyme BcgI (New England Biolabs). This enzyme cuts both upstream and downstream of the 6 bp recognition site, creating fragments of a length of exactly 36 bp with

2 bp overhangs. Adaptors, one of which included degenerate bases to identify PCR duplicates, were ligated and the fragments amplified via 12 cycles of PCR following the protocol provided in Momigliano et al. (2018). From pooled libraries, the target fragments (size about 158-194 bp) were isolated using a BluePippin size selector (Sage Science). Libraries were sequenced on Illumina machines (NextSeq500 and Hiseq 4000) to achieve a mean coverage of approximately 20x. Raw reads were demultiplexed and PCR duplicates were removed as per Momigliano et al. (2018). Any reads that included bases with a Phred quality score <20 were removed. Reads were mapped to the *G. aculeatus* reference genome (release 92) retrieved from the Ensembl database (Hunt et al., 2018) using Bowtie2 (Langmead & Salzberg, 2012). The average alignment rate across samples was 90.84%, with 82.48% of reads aligning to unique positions and 8.36% having multiple hits. SAM files were converted to BAM files and indexed using SAMtools v.1.10 (Li et al., 2009).

For whole genome samples from the Caspian Sea, fresh DNA extracts were prepared from fin clips using a salt extraction protocol (Aljanabi & Martinez, 1997). DNA shearing was performed using a Covaris ultrasonicater with a program targeting 300 bp, and fragment distribution was checked with a High Sensitivity DNA Analyses Kit on a Bioanalyzer 2100 (Agilent). The Truseq V2 Sample Preparation Kit (Illumina) was followed according to the manufacturer's instructions using approximately 1 µg of DNA. Quality and quantity of libraries were assessed on a BioAnalyzer 2100 (Agilent) and a Qubit dsDNA HS Assay (Life Technologies). Libraries were sequenced on an Illumina Hiseq 2000 (paired-end, 150 bp) at the Norwegian Sequencing Centre.

Whole genome sequences were mapped to the *G. aculeatus* reference genome (release 92) using BWA v.0.7.17 (Li & Durbin, 2010) and SAMtools using a custom pipeline (provided by Coll Costa, 2021). Following the conversion of SAM to BAM files, samples with an average read depth below four were removed.

SNP data preparation

For 2b-RAD samples, 11 technical replicates were taken to compile a list of SNPs with high confidence, which were then used to perform Variant Quality Score Recalibration (VQSR),

following GATK best practice (Dixon et al., 2015). Genotypes from 258 samples were hard-called using the GATK v.3.8 functions HaplotypeCaller, CombineGVCFs and GenotypeGVCFs, producing a VCF (Variant Call File). The VCF file was filtered using VCFtools v.0.1.16 (Danecek et al., 2011), by removing indels (*--remove-indels*), triallelic SNPs (*--min-alleles 2 --max-alleles 2*), SNPs with minor allele frequencies below 0.01 (*--maf 0.01*) and more than 10% missing data (*--max-missing 0.9*), retaining loci with a minimum read depth of 5 (*--minDP 5*), a minimum mean depth of 10 (*--min-meanDP 10*), a maximum depth of 500 (*--maxDP 500*), a maximum mean depth of 100 (*--min-meanDP 100*), and excluding variants with quality below 20 (*--minGQ 20*). The final VCF contained 25,125 out of originally 31,438,514 sites. This drastic reduction was driven primarily by our inclusion of both 2b-RAD and whole genome sequencing data, as we retained only SNPs that were covered by both sequencing approaches, hence reducing the whole genome dataset to the bases covered by 2b-RAD.

Genetic diversity and structure

We obtained estimates of nucleotide diversity (π; Nei & Li, 1979) and respective confidence intervals (α = 0.05) from folded one-dimensional bootstrapped site frequency spectra (SFS) obtained with ANGSD v.0.934 (Korneliussen et al., 2014) using a custom script (Momigliano, 2021; https://github.com/Nopaoli/Demographic-Modelling). We calculated allelic differentiation F_{ST} (Weir & Cockerham, 1984), absolute genetic divergence (D_{xy}) and individual observed heterozygosity (H_O) for each chromosome using the *popgenWindows.py* script from the '*genomics_general*' package (Martin, 2018; https://github.com/simonhmartin/genomics_general), and averaged estimates from different chromosomes to obtain a single genome-wide average. D_{xy}, a measure of absolute divergence, was calculated as the average number of per site pairwise differences between sequences from two populations, and, unlike F_{ST}, is not sensitive to current levels of within population diversity (Charlesworth, 1998; Charlesworth et al., 1997; Jakobsson et al., 2013; Nei, 1973), but it does depend on ancestral levels of diversity (Cruickshank & Hahn, 2014). As this is expected to vary broadly across the *G. aculeatus* distribution (Fang et al. 2020a, 2021), we also calculate *dA*, a relative measure of net nucleotide differences between two populations which, assuming

ancestral genetic diversity is well approximated by $\overline{\pi}$, corrects for ancestral diversity according to the formula: $dA = D_{xy} - \left(\frac{\pi_x + \pi_y}{2}\right)$ (Cruickshank & Hahn, 2014; Nei & Li, 1979).

As this analysis requires both variant and invariant sites, the following procedure was carried out to efficiently generate a reduced dataset for which we called genotypes at all sites. We extracted a list of 10,000 genotyped intervals (mostly of 20–36 bp in length, representing single 2b-RAD loci) from the gVCF of the Adriatic sample with the highest average sequencing depth (31.9x) using a custom BCFtools script (https://gist.github.com/ksamuk). This resulted in a list of 257,137 sites across the genome. We then called variants for all 258 samples using the GATK GenotypeGVCFs module, including variant and invariant sites (*-allSites*). The resulting VCF was filtered with VCFtools, removing indels *(--remove-indels*), retaining loci with a minimum read depth of 5 (*--minDP 5*), a minimum mean depth of 10 (*--min-meanDP 10*), a maximum depth of 500 (*--maxDP 500*), a maximum mean depth of 100 (*--min-meanDP 100*), excluding variants with quality below 20 (*--minGQ 20*), excluding sites with more than 10% of missing data (*--max-missing 0.9*) and removing *G. nipponicus* samples. This filtering produced a dataset of 127,334 sites and 254 samples, which was converted into *geno* format (Martin, 2018).

We assessed individual ancestry of 169 *G. aculeatus* individuals across 15 Adriatic freshwater and two marine Atlantic populations by using the model-based program ADMIXTURE v.1.3.0 (Alexander et al., 2009). For the analysis, SNP data restricted to these individuals were pruned for linkage disequilibrium in PLINK v.1.9 (Purcell et al., 2007) in 50 SNP windows with a five SNP window shift, and a r^2 of 0.5. Clusters (K) = 2-20 were tested to determine the optimal number of K by calculating the fivefold cross-validation standard errors in ADMIXTURE. Q estimates for K 2,5,10 and 15 were plotted in R v.4.0.2 (R Core Team, 2020) and R Studio v.1.3.1073 (RStudio Team, 2020) using the R package BITE v.1.2.0008 (Milanesi et al., 2017), admixture plots for the entire range of K are given in Supplementary Figure S1. Geographic structure across all five global regions was explored by performing a Principal Component Analysis (PCA) on a filtered SNP data set (same filters as in genetic diversity and differentiation analysis), as well as by excluding Eastern and Western Pacific regions using SNPRelate v.1.6.4 (Zheng et al., 2012).

Demographic analyses

Population trees with admixture. A maximum likelihood tree with migration events among *Gasterosteus* populations from five geographic regions (Eastern and Western Pacific, Trans-Atlantic, Caspian and Adriatic Sea) was reconstructed using TreeMix v.1.12 which uses allele frequency data and a Gaussian approximation of genetic drift (Pickrell & Pritchard, 2012). The pruned VCF (50 SNP windows with five SNP window shift, $r^2 = 0.5$) excluding sex chromosome 19 was filtered for sites where heterozygosity > 0.6 in at least two populations. The SNP data was converted into the TreeMix input file with STACKS v.2.55 *populations* module (Catchen et al., 2013). First, 500 TreeMix bootstrap replicates were generated with a SNP block size for estimating the covariance matrix set at 100 (*-k*), and *G. nipponicus* set as the outgroup (*-root*), from which a consensus tree was built using PHYLIP v.3.697 (Felsenstein, 2005). To obtain the optimal number of migration events (*m*), TreeMix was run as follows: SNP block size at 100, the consensus tree obtained by PHYLIP set as the starting tree (*-tf*), *m* = 1–10 with 10 iterations for each *m*. The variance of relatedness between populations explained and the change in variance explained by the models were calculated with the R package OptM v.0.1.3 (Fitak, 2018), which suggested an optimum *m* of three. Finally, 30 independent runs from as many random seeds were carried out with three migration edges, 100 SNP blocks, using the consensus tree as a starting point and rooted with *G. nipponicus*. From the resulting trees, we retained the tree with the highest likelihood. Matrices representing residuals and drift estimates, as well as the final tree with migration edges was plotted in R using the BITE package, indicating bootstrap values for each node and migration weight (*w*; Supplementary Figure S2). For each migration event, the least significant p-value recovered across runs, migration weights and errors averaged over 30 final runs were reported (Table 1). Scripts for the TreeMix analysis are available on GitHub (https://github.com/carolindahms/TreeMix).

Changes in N in single populations. Past changes in effective population size (N_e) for each of the 15 Adriatic and two North Sea (SYL and TEX) populations were inferred using the software Stairway Plot v.2 (Liu & Fu, 2015). Stairway plots were derived from folded one-dimensional SFS which were based on genotype likelihoods and site allele frequency likelihoods calculated using ANGSD (*-doSaf1, -GL1*), retaining sites with quality control *(-uniqueOnly 1, -remove_bads 1, -*

minQ 20, -minMapQ 20). Stairway plots were calculated assuming a generation time of two years, including and excluding singletons (for the latter see Supplementary Figure S3), using $\frac{2}{3}$ of the sites for training and four random break points at $\frac{1}{4}, \frac{1}{2}, \frac{2}{3}$ and 1 times the number of samples in each population. The implemented composite likelihood estimations of θ at different epochs were scaled by a mutation rate (μ) of 1×10^{-8} per site per year (Liu et al., 2018). Historical N_e estimations with a μ of 7.1×10^{-9} (Guo et al., 2013) and 3.7×10^{-8} (Liu et al., 2016) are provided in Supplementary Figure S4.

Demographic history of pairs of populations. We reconstructed the demographic history of each pair of the 15 Adriatic populations using the software *moments* v.1.1.0 (Jouganous et al., 2017). The modelling was based on folded two-dimensional SFS calculated with EasySFS (https://github.com/isaacovercast/easySFS) from a VCF excluding variants from chromosome 19, removing sites with heterozygosity > 0.6 across all or at least two populations, with quality below 20 (*--minGQ 20*), allowing no more than 10% missing sites *(--max-missing 0.9*) and keeping one SNP per 2b-RAD locus (*--thin 36*). For each population pair combination four simple models were tested: strict isolation (SI), isolation with migration (IM), ancient migration (AM), secondary contact model (SC), as well as their respective variations that included instantaneous changes in N_e in both daughter populations (SI_{NeC}, IM_{NeC}, AM_{NeC}, SC_{NeC} models) and models with exponential growth (SI_G, IM_G, AM_G, SC_G models) using a custom python pipeline (https://github.com/carolindahms/moments). A graphical representation of all tested models is given in the Supplementary Materials (Figure S5). All models start with an ancestral population of size N_{ANC} that splits into two populations of size N_1 and N_2 at time T_1. The SI model has no migration, while in the IM model migration is continuous and asymmetric. The SC model includes a period of strict isolation starting at time T_1 and a period of secondary contact when asymmetric migration begins at time T_2, while for the AM model the opposite applies (i.e., strict isolation starts at time T_2). The optimization procedure was run as described by Momigliano et al. (2021). In short, the pipeline ran five independent optimization routines each consisting of five optimization rounds with 20–30 iterations each round. For each population pair, we calculated the Akaike Information Criterion (AIC) from the best replicate of each model (AIC= −2(log −likelihood) + 2K, where K is the number parameters) and the $DAIC_i = AIC_i - AIC_{min}$. In cases the best

ranking models were nested, we used a Likelihood Ratio Test to statistically test support for the more complex model, calculating the correct weighting of χ^2 distributions according to Ota et al. (2000). Whenever the best ranking models were not nested, we choose the most complex model when ΔAIC ≥ 7. However, in some cases parameter runaway behaviour (especially at *T* estimations) and over parametrization led to biologically implausible results and/or was approaching a similar model. In cases where T_2 approached the lower boundary of parameter space (1×10^{-3}) or was less than 100 generations, the model was replaced by the next best fitting model (Supplementary Table S2). Plotted residuals and inferred SFS for each model can be found in Supplementary Figure S6.

Parameters estimated in coalescent units were scaled based on estimates of N_{ANC} as outlined in the *dadi* software manual (Gutenkunst et al., 2009). N_{ANC} was calculated as $\frac{\theta}{4L\mu}$, assuming a μ of 1×10^{-8}, and where *L* is the total sequence length from which SNPs used in demographic analyses originated (*L* = 736,970). We calculated *L* as $bases \times \frac{SNPs_{filt}}{SNPs_{raw}}$, where *bases* is the average of sequenced bases across all tested populations, $SNPs_{raw}$ is the total number of SNPs before filtering the SNP data and $SNPs_{filt}$ is the number of SNPs retained after filtering SNP data and which were used to estimate the SFS. Migration rates (m_{12}, m_{21}) were scaled by $2N_{ANC}$, divergence time T_{Div} (the sum of all respective T_1 and T_2 estimates) and time of strict isolation were scaled by $4N_{ANC}$; respective medians (here defined as $\tilde{x}$) and inter-quartile ranges (IQR, the difference between the 3rd and 1st quartile) were computed. We plotted time of strict isolation (in years) only for the AM and SI models, while migration rates (given in proportions of one population being made up of migrants from another population) were divided into recent migration (gene flow estimates only from SC and IM models) and ancient migration (estimates only from AM and IM models). The absolute number of migrants (M_{12}, M_{21}) were calculated for the AM, IM and SC models (excluding exponential growth models) from scaled migration rates and population sizes from the relevant time period. We included only migration estimates higher than one migrant per 100 generations, removing migration rates below this threshold, and suggesting a SI model for populations where both migration estimates (M_{12}, M_{21}) fell below cut-off.

Genetic parallelism

As the extinction of the ancestral marine populations in the Mediterranean Sea rules out the possibility to identify regions under parallel selection exclusive to Adriatic freshwater populations, we aimed to test the extent to which marine-freshwater differentiated genomic regions in the Eastern Pacific and in the Atlantic identified in Fang et al. (2020a) are also involved in freshwater adaptation in the Adriatic Sea populations analysed here. Since a different restriction enzyme was used to build RAD libraries, we could not directly compare marine-freshwater differentiation at the outlier loci identified in Fang et al. (2020a). Instead, we analysed all available data between the first and the last SNP for each region in Fang et al. (2020a), +/- a 100Kbps buffer-zone on each side. Analyses were performed on genotype likelihoods with minimal quality filtering (bi-allelic SNPs with *maf* > 0.01 and a maximum of 70% missing data) to maximise the number of analysed SNPs, resulting in a data set of 39,674 loci. In Fang et al. (2020a), 12 groups of highly correlated sets of loci (LD-clusters) showed significant association with ecotype. However, two of these clusters mapped to more than one distinct genomic region. Therefore, we separated loci in cluster 11 (Chr4) and 20 (Chr20) into three and two regions, respectively (Table 2). Using samples only from the Eastern Pacific and the Atlantic, we first performed linkage disequilibrium network analyses (LDna; Kemppainen et al., 2015; Fang et al., 2020a, 2021) for each genomic region separately. Second, for each nested set of clusters in the resulting single linkage hierarchical clustering tree (where nodes are loci and edges represent the weakest LD-value between any two nodes in the cluster), we regressed the coordinates of the first Principal Component (PC1-score) against ecotype treated as a binary trait [0,1] using the restricted maximum likelihood (REML)-based method EMMAX (Fang et al., 2021; Kang et al., 2010; Li et al., 2018). As such, PC1 compresses the information from all (correlated) SNPs in LD-clusters into "synthetic multi-locus alleles" (SMLAs) with the variance explained determined by how correlated SNPs in the clusters are. To reduce false positives due to relatedness, a relationship matrix was included as a random effect which in Fang et al. (2021) completely reduced p-value inflation in their three-spined stickleback data set from the Atlantic. Third, from the single linkage clustering tree we identified the nested set of loci that was most significantly associated with ecotype (in the Atlantic and the Eastern Pacific; Supplementary Figure S7).

Fourth, based on these loci, we performed PCA analyses to get a secondary set of PC1-scores for all individuals, including the Adriatic freshwater populations (provided that nominal p-value for the most significant LD-cluster was <0.05). These PC1-scores were then scaled between [0,1] and polarized such that the mean score for the marine individuals in the Eastern Pacific and in the Atlantic were lower than for the corresponding freshwater individuals. As such, for genomic regions strongly associated with ecotype, all marine individuals are expected to have low PC1-scores (~0) and all freshwater individuals that have a high frequency of freshwater alleles/haplotypes for a given genomic region are expected to have high scores (~1). The mean PC1-score for a given group of individuals is denoted by *"PC1"* (Supplementary table S3). LD-values (r^2) were estimated from genotype likelihoods using *ngsLD* (Fox et al., 2019) and PC1-scores were based on covariance matrices produced by *PCAngsd* also estimated from genotype likelihoods (Meisner & Albrechtsen, 2018).

RESULTS

Genetic diversity

Both H_O and π varied widely across the sampling area and showed similar patterns (Figure 2a, b). Both diversity measures confirmed diversity to be the lowest in the Adriatic, with Greek populations having the lowest levels of heterozygosity ($\bar{H}_O$ = 3.3 × 10^{-4}, 95% confidence interval (CI): 2.8 × 10^{-4}-3.7 × 10^{-4}) and nucleotide diversity (π = 4 × 10^{-4}, 95% CI: 3.9 × 10^{-4}-4.1 × 10^{-4}) and North Italian the highest H_O ($\bar{H}_O$ = 7 × 10^{-4}, CI: 6.6 × 10^{-4}-7.4 × 10^{-4}). Levels of diversity increased in the Caspian ($\bar{H}_O$ = 1.4 × 10^{-3}, 95% CI: 7 × 10^{-4}-2.1 × 10^{-3}; π = 2.9 × 10^{-3}, 95% CI: 2.8 × 10^{-3}-2.9 × 10^{-3}) and the Atlantic region. The Atlantic marine ecotype had surprisingly lower levels of heterozygosity ($\bar{H}_{Omarine}$ = 1.5 × 10^{-3}, 95% CI: 1.3 × 10^{-3}-1.8 × 10^{-3}) than freshwater conspecifics ($\bar{H}_{Ofreshwater}$ = 2.2 × 10^{-3}, 95% CI: 2.1 × 10^{-3}-2.4 × 10^{-3}), but this pattern was largely driven by two populations (SYL and TEX). Genetic diversity was highest in the Pacific (Figure 2a, b), with Eastern and Western Pacific freshwater populations having the highest levels of heterozygosity ($\bar{H}_O$ = 4.3 × 10^{-3}, 95% CI: 3.9 × 10^{-4}-4.8 × 10^{-3}; $\bar{H}_O$ = 4.4 × 10^{-3}, 95% CI: 2.5 × 10^{-3}-6.2 × 10^{-3}, respectively) and nucleotide diversity (π = 4.2 × 10^{-3}, 95% CI: 4.1 × 10^{-3}-4.3 × 10^{-4}; π = 4.62 × 10^{-3}, 95% CI: 4.6 × 10^{-3}-4.63 × 10^{-3}, respectively).

Genetic differentiation

We identified clear differences in the extent of population differentiation (F_{ST}) within and between geographic regions (Figure 3a). Three clusters of very low pairwise F_{ST} stood out: the marine Eastern Pacific populations, Western Pacific and the Trans-Atlantic populations irrespective of ecotype (Figure 3a). In the Adriatic, despite some heterogeneity, levels of genetic differentiation were very high with a mean F_{ST} of 0.45 (±0.17). Pairwise F_{ST} among Italian populations were relatively low, whereas Greek and Albanian populations showed extremely high F_{ST} values ranging from 0.5 to 0.8 (Figure 3a).

D_{xy} provided further evidence for global heterogeneity in levels of divergence (Figure 3b). Absolute divergence was highest within the Pacific ($\bar{D}_{xy} = 5.2 \times 10^{-3} \pm 1 \times 10^{-4}$), particularly within freshwater populations from Vancouver Island (CA_R and CA_L; Figure 3b). Absolute divergence was reduced within the Trans-Atlantic region ($\bar{D}_{xy} = 2.5 \times 10^{-3} \pm 3.5 \times 10^{-5}$), while pairwise values of D_{xy} within the Adriatic region showed the lowest values ($\bar{D}_{xy} = 1.4 \times 10^{-3} \pm 1.6 \times 10^{-5}$; Figure 3b). Within the Adriatic Sea region, the Italian sub-region had notably lower levels of divergence (e.g., IBO and IPI), while Greek and Albanian populations, especially GM, stood out with higher levels of divergence (Figure 3d).

dA estimates also suggested distinct patterns of divergence among geographic regions (Figure 3c). Clusters of low degree of divergence emerged within the Pacific ($\bar{dA} = 1 \times 10^{-3} \pm 1 \times 10^{-4}$), Trans-Atlantic ($\bar{dA} = 1 \times 10^{-3} \pm 2.1 \times 10^{-5}$) and some Adriatic (Italian) populations (Figure 3c). Mean *dA* for the Adriatic sticklebacks was 9×10^{-4} ($\pm 2.1 \times 10^{-5}$), with Greek and Albanian populations, especially GM, showing deeper divergence from other populations (Figure 3c).

Population structure

The PCA showed strong differentiation of the Eastern Pacific from the rest of the world along PC1, with freshwater populations being extremely separated from all other populations (Figure 4a). Individuals from the Western Pacific clustered closer to EP marine individuals and were distinct from European populations along the PC1 axis (Figure 4a). Removal of the Pacific populations revealed further structure among the Trans-Atlantic, Adriatic and Caspian populations (Figure 4b). Two main clusters formed in the PC2 axis accounting for a large

difference between one Greek lineage (GM) and the rest. While PC1 represented variation among the Trans-Atlantic populations, another Greek lineage (GF) separated from the rest of the Adriatic population and clustered together with Caspian and marine North Sea (TY_M) populations along the 1st dimension (Figure 4b).

The admixture analysis suggested that structure of the data was best explained with 15 clusters (K = 15) based on cross-validated standard errors (Figure 4c). At K = 2, admixture was almost absent - Italian populations were grouped together, while Albania and Greece grouped with the two marine samples from the North Sea (SYL and TEX). K = 5 identified multiple separate groupings, clustering GF with marine populations, whereas some Italian populations (ILA and IRB) showed signs of admixture from Albania, and the Greek population GM showed admixture from Italy and the North Sea (SYL; Figure 4c). At K = 10, populations aligned into multiple groups with almost no admixture, except IRB and ILA. At K = 15, each population, except for marine individuals, grouped separately with almost no signs of admixture except in one Italian population (IRE; Figure 4c).

Demographic history

All final (n = 30) runs with three migration events in TreeMix reached the same maximum likelihood value [ln(likelihood) = 3819.97], with the final tree explaining 99.39% of the variance in relatedness between populations (Figure 4d). Where nodes did not have bootstrap values, TreeMix slightly changed the topology of the consensus tree. The tree placed the oldest lineages in the Pacific, where the longest tree branch between the Pacific and the rest of the world indicated high levels of drift (Figure 4d). One clade represented the Trans-Atlantic region, further separating two North Sea populations (SYL and TEX) from the Baltic Sea (GER_R, GER_L), Labrador Sea (Kob_M, Kob_L, Qar_L) and the rest of North Sea populations (TY_M, TY_F, NOR_R, NOR_L; Figure 4d). A second clade represented southern Europe, splitting into one Greek (GF) lineage and another subclade separating central Italian populations (ISA, IGI, ICL) from the rest (Greek, Caspian, the less divergent northern Italian and one central Italian population ILA; Figure 4d). Notably, Greek (GM, GAC) and Albanian (AD) populations maintained higher levels of drift compared to the rest of southern Europe (Figure 4d, Supplementary Figure S2). Migration events (labelled I-III) were all significant ($p < 0.05$) and had generally low migration weight, with

recipients in the Trans-Atlantic (I, w = 0.12), Caspian Sea (II, w = 0.06) and Caspian-Greek populations (III, w = 0.03; Table 1).

In the stairway plot analysis, inclusion of singletons provided clearer resolution in differences of N_e changes between populations (Supplementary Figure S3). Most of the Adriatic three-spined stickleback populations have experienced bottlenecks, with current N_e sizes estimated to be very small, mostly ranging between only few dozens to 5,000 individuals (Figure 5a-d). Only one Greek lineage (GF) remained stable at larger sizes (N_e ~12,000), and one Italian population (IBO, N_e ~12,000) expanded after a bottleneck around 6 kya (Figure 5c). The Greek populations had some of the lowest N_e estimates, as low as 20 in GP and GM (Figure 5b). The demographic trends observed in the Adriatic were clearly different from marine North European populations (SYL and TEX), that have experienced population expansions around 38 and 15 kya, reaching N_e sizes of around 45,000 and 75,000, respectively (Figure 5e).

The best demographic models inferred by *moments* indicated generally high similarity between observed and expected allele frequency spectra, i.e., residuals were very low and normally distributed suggesting good model fit (Supplementary Figure S6). Prevalence of demographic scenarios among Adriatic sticklebacks was approximately equal (25–30%), except the SI model which was the least common (8%), occurring mostly in the Albanian population (AD; Figure 6a). Time of divergence ranged from a few hundred to over one hundred thousand years, $\tilde{T}_{DIV}$ = 55,653 (IQR = 50,966). The deepest divergence was estimated between Greek and northern Italian ($\tilde{T}_{DIV}$ = 87,757, IQR = 68,142), and within Greek populations ($\tilde{T}_{DIV}$ = 66,770, IQR = 50,441), while the most recent divergence times were within northern Italian ($\tilde{T}_{DIV}$ = 9,694, IQR = 45,630) and between Albanian and northern Italian populations ($\tilde{T}_{DIV}$ = 36,764, IQR = 12,087; Figure 6b). Ancient gene flow (estimated by the AM model) ended around 3,859 years ago (IQR = 4,703), with the longest periods of isolation occurring in Albanian and Greek (GM, GS) populations (Figure 6b). Recent and ancient migration in the Adriatic was overall low ($\tilde{m}_{recentt}$ = 8.6 × 10^{-6}, IQR = 5.8 × 10^{-5}; $\tilde{m}_{ancient}$ = 9.6 × 10^{-6}, IQR = 1.9 × 10^{-5}); with m_{12} representing the proportion of individuals in the first population made up of immigrants from the second population and *vice versa* for m_{21}. Highest migration rates occurred in Italy, to a higher degree within (e.g., IGI-ILA, IRI-IRE) than between regions (Figure 6c, d). Absolute numbers of migrants were low ($\tilde{M}_{recent}$ =

0.02, IQR = 0.02; $\bar{M}_{ancient}$ = 0.06, IQR = 0.16; Figure 6e, f). In around 50% of population pairs with migration scenarios (excluding exponential growth models) at least one *M* estimate was lower than one migrant per 100 generations and in four pairs involving Greek GM and GS populations both migration estimates (M_{12}, M_{21}) were below this threshold (Figure 6a).

Genetic parallelism

Among the 15 outlier regions analysed from Fang et al. (2020a), nine were also significantly associated with marine freshwater differentiation here (Table 2; Figure 7). In the Eastern Pacific, PC1-scores were high among freshwater samples for all genomic regions (*PC1* = [0.34,0.950]) except Chr20_2 (*PC1* = 0.079) and in the Atlantic this was the case for all (*PC1* = [0.42,1]) except Chr4_5 (*PC1* = 0.16) and Chr8_1 (*PC1* = 0.12). Among marine samples, PC1-scores were generally low for all genomic regions in the Eastern Pacific (Table 2). In contrast, for several genomic regions (e.g., Chr1_2, Chr4_6 and Chr9_1) Atlantic marine individuals also tended to group with the freshwater individuals (i.e., have high PC1-scores). In the south, Adriatic samples clustered with freshwater samples from the Eastern Pacific and Atlantic for five out of the 15 analysed outlier genomic regions (Chr1_2, Chr4_3, Chr4_6, Chr9_1 and Chr20_1), with PC1-scores close to 1 (Table 2). This was the case for only one region in the Caspian Sea and in the Western Pacific, which in both cases involved Chr9_1.

DISCUSSION

The aim of this study was to investigate the demographic factors shaping standing genetic variation (SGV) in three-spined stickleback freshwater populations from the Adriatic Sea basin, and their influence on the probability of parallel evolution. The results suggested that freshwater populations surrounding the Adriatic Sea have experienced recent population size bottlenecks and are to the greatest extent currently isolated and highly differentiated. They also exhibit very low genetic diversity and their evolutionary origin pre-dates the last glacial maximum. Although the degree of genetic parallelism in the Adriatic Sea populations was lower compared to parallelism detected in freshwater populations elsewhere in the world, multiple genomic regions were significantly associated with parallel freshwater adaptation in the Adriatic Sea region. Plausible hypothesis explaining these findings are discussed further in this section.

The results indicate that the Adriatic three-spined sticklebacks have very low or absent gene flow and maintain exceptionally high levels of genetic differentiation (F_{ST}) and low genetic diversity. Comparatively low absolute divergence (D_{xy}) in the Adriatic suggests that high F_{ST} is driven by a loss of within population diversity (Charlesworth, 1998; Charlesworth et al., 1997; Jakobsson et al., 2013), rather than divergence, i.e., accumulation of mutations through time. Rapid drift could have increased differentiation, while the relatively short time of divergence between Adriatic populations compared to other global regions may have resulted in reduced *dA* (Cruickshank & Hahn, 2014; Nei & Li, 1979). These findings support previous studies suggesting extended periods of isolation and drift in the Mediterranean populations (DeFaveri et al., 2012; Mäkinen & Merilä, 2008).

A certain degree of heterogeneity in diversity and genetic differentiation among the Adriatic three-spined sticklebacks could be explained by their differing demographic histories. In accordance with the assumption that historical N_e changes are expected to govern the likelihood of genetic drift eradicating or fixing genetic variants (Hedrick, 2005), Adriatic populations with larger N_e have generally lower levels of genetic differentiation. Greek populations, such as the very small and isolated spring population GM, which have experienced multiple bottlenecks resulting in very low current N_e, show generally higher pairwise F_{ST} compared to Italian populations as a likely result of genetic diversity loss. Higher diversity in the Italian sub-regions could be explained by their two separate – Tyrrhenian (ICL) and Adriatic (all other Italian populations) – regions of origin. Another explanation could be the elevated degree of gene flow supplying novel genetic variation, likely due to the closer geographical proximity of Italian populations as compared to other Adriatic populations. This inference was also supported by genetic ancestry analyses: there was evidence of admixture only among northern Italian populations (e.g., IRI and IRE) and between neighbouring Italian sub-regions. The high prevalence of secondary contact models in these sub-regions provides further independent evidence of recent admixture, whereas the time of strict isolation appeared to be longest in Greek and Albanian populations.

Heterogeneity in differentiation within the Adriatic region was also reflected in the high variance in divergence estimates. For example, Italian populations share a more recent ancestry

than Greek and Albanian populations, meaning that the lower pairwise F_{ST} values observed in this region could also be a result of very recent divergence. On the other hand, Greece hosts some of the most divergent populations such as GM, which PCA identified as the most genetically distant from all other southern European and Atlantic populations. This is consistent with the high respective D_{xy} and divergence time estimates, suggesting a more ancient and distinct origin of the GM lineage. Divergence time estimates (maxT_{DIV} = 150,853 years, $\tilde{T}_{DIV}$ = 55,653, IQR = 50,966) obtained by demographic modelling are in line with the results of Fang et al. (2020b), falling between the suggested Pacific-Atlantic divergence time (29.5–226.6 kya) and time to the most recent common ancestor of the younger North European lineages (11.3–96.2 kya). Another Greek population (GF) formed a separate lineage (Figure 4d) and clustered with a marine North Sea population (Figure 4b), which could imply that GF harbours ancestral variation of one of the lineages that colonized Northern Europe following the retreat of ice sheets around 10 kya.

Differences in the degree of divergence among Adriatic three-spined sticklebacks might suggest that some of the older lineages, which likely emerged from more ancient freshwater colonization events (Cano et al., 2008; DeFaveri et al., 2012; Mäkinen & Merilä, 2008), stem from a distinct colonization wave from the Eastern Pacific hundreds of thousands of years ago, whereas younger lineages originated from a more recent migration wave to the Mediterranean Sea. Considering the dynamic nature of marine populations, the more divergent lineages (Greek, Albanian) could have originated from marine populations significantly different from those ancestral populations of less divergent (Italian) populations, meaning that different Adriatic sub-regions could have had access to different sources of SGV. Moreover, deeper divergence from a common ancestor is likely to decrease the probability of genetic parallelism, as the pool of SGV is more likely to diverge over time (Conte et al., 2012), which would predict differing patterns of parallel evolution between lineages diverged pre- and post-glacially.

Compared to freshwater populations elsewhere in the world, the levels of genetic parallelism in the Adriatic Sea basin populations are considerably lower (Figure 7, Supplementary Table S3). There are two possible and mutually non-exclusive explanations for this. First, since the likelihood of parallel genetic changes in response to similar selection pressures depend on the pool of SGV feeding the adaptative process, heterogeneity in the pool of SGV that fed

freshwater colonization in the Adriatic basin populations might have been greater than elsewhere where most freshwater populations are still (or have been recently) connected to marine populations. This interpretation is supported by TreeMix which showed that within the monophyletic Adriatic radiation, there are old distinct or monophyletic subclades (GM, GF), which could also have contributed to generally smaller PC1-score differences between marine and freshwater samples for genomic regions associated with parallelism in Greek compared with Italian populations (Figure 7, Supplementary Table S3). Therefore, if the ancestors of these subclades were already highly differentiated from each other, this would act to reduce degree of genetic parallelism across the Adriatic Sea.

Second, the low degree of genetic parallelism among freshwater populations around the Adriatic basin could also be explained by heterogenous selection pressures. For instance, if the freshwater habitats, and therefore also selection pressures, are more diversified in the Adriatic region than elsewhere in the world, this would be expected to lead to a low degree of parallelism. This theory is supported by studies attributing differences in genetic parallelism among freshwater sticklebacks at least partially to environmental variation (Magalhaes et al., 2021; Stuart et al., 2017). While this possibility is hard to dismiss in the absence of direct measurement of selection pressures (or habitat diversity), the fact that a much higher degree of parallelism is seen over much wider geographic, climatic, and ecological gradients from California to Alaska in analyses of Eastern Pacific stickleback populations (Fang et al., 2020a) speaks against this explanation. Furthermore, each of the Adriatic Sea basin populations inhabits a relatively small geographic area and shows similar phenotypic indicators of freshwater adaptation (Zanella et al. 2012; but see Zanella et al. 2009) to other freshwater adapted populations elsewhere in the world. Likewise, the much younger radiation in the Atlantic Sea basin also shows a substantially higher degree of genetic parallelism compared to the Adriatic radiation. Again, the Trans-Atlantic radiation covers a range from the Baltic to the Labrador Sea, and hence likely includes a more diverse set of freshwater habitats than the Adriatic basin radiation. In fact, we found that those genomic regions that have high PC1 scores (i.e., approaching the freshwater ecotype) among the Trans-Atlantic marine samples tend to also be those that are geographically widespread (Table 2, Figure 7), which is consistent with the transporter hypothesis and suggests weak selection pressures against freshwater-adapted alleles. Hence, while possible, diversified selection

pressures are an unlikely explanation for the low degree of genetic parallelism in the Adriatic Sea. We consider that heterogeneity in SGV and a lack of gene flow between the (now absent) marine ancestral population and present-day freshwater populations, combined with rapid drift, provide a more likely explanation for the observed patterns. Similar reasoning was recently provided also for the lower degree of parallelism in the Atlantic compared to the Pacific Ocean basin and backed up by simulations (Fang et al. 2020a).

We found only nine out of 15 genomic regions from Fang et al. (2020a) to be significantly associated with ecotype in the Eastern Pacific and Atlantic in our analyses, which could be explained by the fact that the number of SNPs analysed in this study was less than 25% of those analysed in Fang et al. (2020a), and considering the minimal filtering performed on our data set, the effective number of high-quality loci could be even smaller. There was a strong negative correlation (r^2 = 0.78, p = 1.24e-05) between the size of the genomic region (in bps) and the strength of the marine-freshwater association (-log10[P]). This indicates that our analyses are limited by the SNP density, i.e., not enough loci linked to any causal loci were likely available for our analyses to show strong association with ecotype from the smallest genomic regions (containing as few as two marine-freshwater associated SNPs; Table 2). However, this methodological difference should not have biased our findings of lower degree of genetic parallelism in the Adriatic region, as it affected the Atlantic and Pacific regions in a similar fashion. Moreover, some degree of parallelism in the Adriatic might have remained undetected as it was not possible to identify loci involved in parallel freshwater adaptation exclusively in the Adriatic freshwater populations. The absence of any extant individuals representing the ancestral marine population from the Mediterranean precluded our ability to differentiate parallel evolution from genetic drift as drivers for the fixation of specific alleles in multiple Adriatic freshwater populations.

The degree of parallel evolution in the Adriatic Sea was lower than other geographic regions, yet higher than expected given the high genetic differentiation of Adriatic populations and lack of access to a shared pool of SGV. PC1 scores were high in multiple genomic regions such as chromosomes one and four, which are known to mediate freshwater adaptation in three-spined sticklebacks (Jones et al., 2012). This observation could be explained by the following: first, the ancestral marine populations that once resided in the Adriatic Sea harboured high

genetic diversity and transported freshwater-adapted alleles in high frequencies upon freshwater colonization; and second, the loss of diversity in Adriatic freshwater populations occurred after their adaptation to freshwater habitat. Gene flow in populations with the demographic AM scenario was estimated to end only around 3700 years ago (time of strict isolation constituting on average less than $1/10^{th}$ of the total divergence time), which might suggest that freshwater populations had access to a common marine gene pool for a timeframe long enough for gene flow to supply high levels of beneficial alleles, facilitating freshwater adaptation. Coupled with favourable conditions for adaptation, such as high selection pressures, large ancestral N_e ($\tilde{N}_{ANC}$ = 13,818, IQR = 11,148) and initial daughter N_e sizes (5–15 thousand, Figure 5), this scenario could have allowed rapid freshwater colonization and the upkeep of high genetic diversity. After the extinction of marine Mediterranean three-spined sticklebacks, access to SGV ceased and freshwater populations were effectively isolated, i.e., exchanging likely less than seven migrants per 100 generations. The effects of depleted gene flow and bottlenecks from this point were likely to take hold, resulting in heterogenous patterns of high differentiation and low genetic diversity observed among the different Adriatic Sea lineages at the present time.

In conclusion, we demonstrated that signatures of genetic parallelism in response to freshwater adaptation might still be recovered in bottlenecked populations despite high drift and cessation of gene flow, such as in the Adriatic stickleback populations. Our findings suggest that although rapid parallel freshwater adaptation could have occurred before the Mediterranean marine population went extinct, likely multiple factors, such as loss of continuous access to SGV and varying demographic histories and divergent ancestries have generated high heterogeneity in genetic parallelism in the Adriatic region. As our analyses were restricted to north-eastern Mediterranean regions at low SNP density, a more conclusive understanding on the causes of heterogeneity in parallelism among Mediterranean three-spined stickleback lineages could benefit from further analysis combining all geographic regions investigated to date.

ACKNOWLEDGEMENTS

We thank all who provided and helped collect the samples analysed in this study: Asbjørn Vøllestad, Björn Stelbrink, Jacquelin DeFaveri, Jörg Freyhof, Lisa N. S. Shama, Radek Šanda, Sanne Boessenkool, Spase Shumka, Stamatis Zogaris and Theo Bakker. Minnastiina Issakainen is

thanked for DNA extractions. Our research was supported by Academy of Finland (grant numbers 129662, 134728 and 218343 to J.M. and 316294 to P.M.). Sequence data of the Caspian samples was provided by Sanne Boessenkool and Leif Asbjørn Vøllestad, funded by the Research Council of Norway (grant number 16639/F20 awarded to Leif Asbjørn Vøllestad). We thank Massimo Lorenzoni who provided guidance and support for the Italian stickleback sampling. The fish sampling protocols have been established in compliance with the ethical standards, as approved by the Italian regulations and by local permitting authorities who provided the fish sampling authorizations (authorities and permit numbers: Pescara Province, n. 396505 of 12/11/2015; L'Aquila Province, n. 63722 of 24/11/2015; Padova Province, n. 18583 of 03/02/2016; Vicenza Province, n. 275 of 05/04/2016; Umbria Region, n. 2967 of 19/04/2016; Gargano National Park, n. 22/3° of 22/06/2016).

REFERENCES

Alexander, D. H., Novembre, J., & Lange, K. (2009). Fast model-based estimation of ancestry in unrelated individuals. *Genome Research*, *19*(9), 1655-1664.

Aljanabi, S. M., & Martinez, I. (1997). Universal and rapid salt-extraction of high quality genomic DNA for PCR-based techniques. *Nucleic Acids Research*, *25*(22), 4692-4693.

Araguas, R. M., Vidal, O., Pla, C., & Sanz, N. (2012). High genetic diversity of the endangered Iberian three-spined stickleback (Gasterosteus aculeatus) at the Mediterranean edge of its range. *Freshwater Biology*, *57*(1), 143-154.

Arendt, J., & Reznick, D. (2008). Convergence and parallelism reconsidered: what have we learned about the genetics of adaptation? *Trends in Ecology & Evolution*, *23*(1), 26-32.

Arnold, S. J. (1992). Constraints on phenotypic evolution. *The American Naturalist*, *140*, S85-S107.

Bailey, S. F., Blanquart, F., Bataillon, T., & Kassen, R. (2017). What drives parallel evolution? How population size and mutational variation contribute to repeated evolution. *BioEssays*, *39*(1), 1-9.

Barrett, R. D., & Schluter, D. (2008). Adaptation from standing genetic variation. *Trends in Ecology & Evolution*, *23*(1), 38-44.

Barton, N. H., & Charlesworth, B. (1984). Genetic revolutions, founder effects, and speciation. *Annual Review of Ecology and Systematics*, *15*(1), 133-164.

Betancur, R., Ortí, G., & Pyron, R. A. (2015). Fossil-based comparative analyses reveal ancient marine ancestry erased by extinction in ray-finned fishes. *Ecology Letters*, *18*(5), 441-450.

Cano, J. M., Mäkinen, H. S., Leinonen, T., Freyhof, J., & Merilä, J. (2008). Extreme neutral genetic and morphological divergence supports classification of Adriatic three-spined stickleback (Gasterosteus aculeatus) populations as distinct conservation units. *Biological Conservation*, *141*(4), 1055-1066.

Catchen, J., Hohenlohe, P. A., Bassham, S., Amores, A., & Cresko, W. A. (2013). Stacks: an analysis tool set for population genomics. *Molecular Ecology*, *22*(11), 3124-3140.

Charlesworth, B. (1998). Measures of divergence between populations and the effect of forces that reduce variability. *Molecular Biology and Evolution*, *15*(5), 538-543.

Charlesworth, B., Nordborg, M., & Charlesworth, D. (1997). The effects of local selection, balanced polymorphism and background selection on equilibrium patterns of genetic diversity in subdivided populations. *Genetics Research*, *70*(2), 155-174.

Conte, G. L., Arnegard, M. E., Peichel, C. L., & Schluter, D. (2012). The probability of genetic parallelism and convergence in natural populations. *Proceedings of the Royal Society B: Biological Sciences*, *279*(1749), 5039-5047.

Crivelli, A. J., & Britton, R. H. (1987). Life history adaptations of Gasterosteus aculeatus in a Mediterranean wetland. *Environmental Biology of Fishes*, *18*(2), 109-125.

Cruickshank, T. E., & Hahn, M. W. (2014). Reanalysis suggests that genomic islands of speciation are due to reduced diversity, not reduced gene flow. *Molecular Ecology*, *23*(13), 3133-3157.

Danecek, P., Auton, A., Abecasis, G., Albers, C. A., Banks, E., DePristo, M. A., Handsaker, R. E., Lunter, G., Marth, G. T., & Sherry, S. T. (2011). The variant call format and VCFtools. *Bioinformatics*, *27*(15), 2156-2158.

DeFaveri, J., Zanella, L., Zanella, D., Mrakovčić, M., & Merilä, J. (2012). Phylogeography of isolated freshwater three-spined stickleback Gasterosteus aculeatus populations in the Adriatic Sea basin. *Journal of Fish Biology*, *80*(1), 61-85.

Dixon, J. R., Jung, I., Selvaraj, S., Shen, Y., Antosiewicz-Bourget, J. E., Lee, A. Y., Ye, Z., Kim, A., Rajagopal, N., & Xie, W. (2015). Chromatin architecture reorganization during stem cell differentiation. *Nature*, *518*(7539), 331-336.

Fang, B., Merilä, J., Ribeiro, F., Alexandre, C. M., & Momigliano, P. (2018). Worldwide phylogeny of three-spined sticklebacks. *Molecular Phylogenetics and Evolution*, *127*, 613-625.

Fang, B., Kemppainen, P., Momigliano, P., Feng, X., & Merilä, J. (2020a). On the causes of geographically heterogeneous parallel evolution in sticklebacks. *Nature Ecology & Evolution*, *4*(8), 1105-1115.

Fang, B., Merilä, J., Matschiner, M., & Momigliano, P. (2020b). Estimating uncertainty in divergence times among three-spined stickleback clades using the multispecies coalescent. *Molecular Phylogenetics and Evolution*, *142*, 106646.

Fang, B., Kemppainen, P., Momigliano, P., & Merilä, J. (2021). Population structure limits parallel evolution in sticklebacks. *Molecular Biology and Evolution*. https://doi.org/10.1093/molbev/msab144

Felsenstein, J. (2005). *PHYLIP (Phylogeny Inference Package). Version 3.6*.

Ferchaud, A. L., & Hansen, M. M. (2016). The impact of selection, gene flow and demographic history on heterogeneous genomic divergence: Three-spine sticklebacks in divergent environments. *Molecular Ecology*, *25*(1), 238-259.

Feulner, P. G., Chain, F. J., Panchal, M., Huang, Y., Eizaguirre, C., Kalbe, M., Lenz, T. L., Samonte, I. E., Stoll, M., & Bornberg-Bauer, E. (2015). Genomics of divergence along a continuum of parapatric population differentiation. *PLoS Genetics*, *11*(2), e1004966.

Fitak, R. R. (2018). (submitted). optM: an R package to optimize the number of migration edges using threshold models. *Journal of Heredity*.

Fox, E. A., Wright, A. E., Fumagalli, M., & Vieira, F. G. (2019). ngsLD: evaluating linkage disequilibrium using genotype likelihoods. *Bioinformatics*, *35*(19), 3855-3856.

Gienapp, P., Teplitsky, C., Alho, J., Mills, J., & Merilä, J. (2008). Climate change and evolution: disentangling environmental and genetic responses. *Molecular Ecology*, *17*(1), 167-178.

Gomulkiewicz, R., Holt, R. D., & Barfield, M. (1999). The effects of density dependence and immigration on local adaptation and niche evolution in a black-hole sink environment. *Theoretical Population Biology*, *55*(3), 283-296.

Guo, B., Chain, F. J., Bornberg-Bauer, E., Leder, E. H., & Merilä, J. (2013). Genomic divergence between nine-and three-spined sticklebacks. *BMC Genomics*, *14*(1), 1-11.

Guo, B., Fang, B., Shikano, T., Momigliano, P., Wang, C., Kravchenko, A., & Merilä, J. (2019). A phylogenomic perspective on diversity, hybridization and evolutionary affinities in the stickleback genus Pungitius. *Molecular Ecology*, *28*(17), 4046-4064.

Gutenkunst, R. N., Hernandez, R. D., Williamson, S. H., & Bustamante, C. D. (2009). Inferring the joint demographic history of multiple populations from multidimensional SNP frequency data. *PLoS Genetics*, *5*(10), e1000695.

Hedrick, P. W. (2005). A standardized genetic differentiation measure. *Evolution*, *59*(8), 1633-1638.

Hughes, A. L. (1999). *Adaptive evolution of genes and genomes*. Oxford University Press, USA.

Hunt, S. E., McLaren, W., Gil, L., Thormann, A., Schuilenburg, H., Sheppard, D., Parton, A., Armean, I. M., Trevanion, S. J., & Flicek, P. (2018). Ensembl variation resources. *Database*, *2018*.

Jakobsson, M., Edge, M. D., & Rosenberg, N. A. (2013). The relationship between F ST and the frequency of the most frequent allele. *Genetics*, *193*(2), 515-528.

Jones, F. C., Grabherr, M. G., Chan, Y. F., Russell, P., Mauceli, E., Johnson, J., Swofford, R., Pirun, M., Zody, M. C., & White, S. (2012). The genomic basis of adaptive evolution in threespine sticklebacks. *Nature*, *484*(7392), 55-61.

Jouganous, J., Long, W., Ragsdale, A. P., & Gravel, S. (2017). Inferring the joint demographic history of multiple populations: beyond the diffusion approximation. *Genetics*, *206*(3), 1549-1567.

Kang, H. M., Sul, J. H., Service, S. K., Zaitlen, N. A., Kong, S.-y., Freimer, N. B., Sabatti, C., & Eskin, E. (2010). Variance component model to account for sample structure in genome-wide association studies. *Nature Genetics*, *42*(4), 348-354.

Kemppainen, P., Knight, C. G., Sarma, D. K., Hlaing, T., Prakash, A., Maung Maung, Y. N., Somboon, P., Mahanta, J., & Walton, C. (2015). Linkage disequilibrium network analysis (LDna) gives a global view of chromosomal inversions, local adaptation and geographic structure. *Molecular Ecology Resources*, *15*(5), 1031-1045.

Kemppainen, P., Li, Z., Rastas, P., Löytynoja, A., Fang, B., Yang, J., Guo, B., Shikano, T., & Merilä, J. (2021). Genetic population structure constrains local adaptation in sticklebacks. *Molecular Ecology*, *30*(9), 1946-1961.

Kirkpatrick, M., & Peischl, S. (2013). Evolutionary rescue by beneficial mutations in environments that change in space and time. *Philosophical Transactions of the Royal Society B: Biological Sciences*, *368*(1610), 20120082.

Kitano, J., Ross, J. A., Mori, S., Kume, M., Jones, F. C., Chan, Y. F., Absher, D. M., Grimwood, J., Schmutz, J., & Myers, R. M. (2009). A role for a neo-sex chromosome in stickleback speciation. *Nature*, *461*(7267), 1079-1083.

Korneliussen, T. S., Albrechtsen, A., & Nielsen, R. (2014). ANGSD: analysis of next generation sequencing data. *BMC bioinformatics*, *15*(1), 1-13.

Lanfear, R., Kokko, H., & Eyre-Walker, A. (2014). Population size and the rate of evolution. *Trends in Ecology & Evolution*, *29*(1), 33-41.

Langmead, B., & Salzberg, S. L. (2012). Fast gapped-read alignment with Bowtie 2. *Nature Methods*, *9*(4), 357.

Lee, K. M., & Coop, G. (2017). Distinguishing among modes of convergent adaptation using population genomic data. *Genetics*, *207*(4), 1591-1619.

Leinonen, T., McCairns, R. S., O'hara, R. B., & Merilä, J. (2013). Q ST–F ST comparisons: evolutionary and ecological insights from genomic heterogeneity. *Nature Reviews Genetics*, *14*(3), 179-190.

Lenormand, T. (2002). Gene flow and the limits to natural selection. *Trends in Ecology & Evolution*, *17*(4), 183-189.

Li, H., & Durbin, R. (2010). Fast and accurate long-read alignment with Burrows–Wheeler transform. *Bioinformatics*, *26*(5), 589-595.

Li, H., Handsaker, B., Wysoker, A., Fennell, T., Ruan, J., Homer, N., Marth, G., Abecasis, G., & Durbin, R. (2009). The sequence alignment/map format and SAMtools. *Bioinformatics*, *25*(16), 2078-2079.

Li, Z., Kemppainen, P., Rastas, P., & Merilä, J. (2018). Linkage disequilibrium clustering-based approach for association mapping with tightly linked genomewide data. *Molecular Ecology Resources*, *18*(4), 809-824.

Liu, S., Ferchaud, A.-L., Grønkjær, P., Nygaard, R., & Hansen, M. M. (2018). Genomic parallelism and lack thereof in contrasting systems of three-spined sticklebacks. *Molecular Ecology*, *27*(23), 4725-4743.

Liu, S., Hansen, M. M., & Jacobsen, M. W. (2016). Region-wide and ecotype-specific differences in demographic histories of threespine stickleback populations, estimated from whole genome sequences. *Molecular Ecology*, *25*(20), 5187-5202.

Liu, X., & Fu, Y. X. (2015). Exploring population size changes using SNP frequency spectra. *Nature Genetics*, *47*(5), 555-559.

Lucek, K., & Seehausen, O. (2015). Distinctive insular forms of threespine stickleback (Gasterosteus aculeatus) from western Mediterranean islands. *Conservation Genetics*, *16*(6), 1319-1333.

Lynch, M., & Walsh, B. (1998). *Genetics and analysis of quantitative traits* (Vol. 1). Sinauer Sunderland, MA.

MacPherson, A., & Nuismer, S. (2017). The probability of parallel genetic evolution from standing genetic variation. *Journal of Evolutionary Biology*, *30*(2), 326-337.

Magalhaes, I. S., Whiting, J. R., D'Agostino, D., Hohenlohe, P. A., Mahmud, M., Bell, M. A., Skúlason, S., & MacColl, A. D. (2021). Intercontinental genomic parallelism in multiple three-spined stickleback adaptive radiations. *Nature Ecology & Evolution*, *5*(2), 251-261.

Marques, D. A., Meier, J. I., & Seehausen, O. (2019). A combinatorial view on speciation and adaptive radiation. *Trends in Ecology & Evolution*, *34*(6), 531-544.

Matschiner, M., Hanel, R., & Salzburger, W. (2011). On the origin and trigger of the notothenioid adaptive radiation. *PLoS One*, *6*(4), e18911.

Mayr, E. (1963). *Animal Species and Evolution*. Harvard University Press.

Meisner, J., & Albrechtsen, A. (2018). Inferring population structure and admixture proportions in low-depth NGS data. *Genetics*, *210*(2), 719-731.

Merilä, J., & Crnokrak, P. (2001). Comparison of genetic differentiation at marker loci and quantitative traits. *Journal of Evolutionary Biology*, *14*(6), 892-903.

Milanesi, M., Capomaccio, S., Vajana, E., Bomba, L., Garcia, J. F., Ajmone-Marsan, P., & Colli, L. (2017). BITE: an R package for biodiversity analyses. *bioRxiv*, 181610. https://doi.org/10.1101/181610

Momigliano, P., Denys, G. P., Jokinen, H., & Merilä, J. (2018). Platichthys solemdali sp. nov.(Actinopterygii, Pleuronectiformes): a new flounder species from the Baltic Sea. *Frontiers in Marine Science*, *5*, 225.

Momigliano, P., Florin, A. B., & Merilä, J. (2021). Biases in demographic modelling affect our understanding of recent divergence. *Molecular Biology and Evolution*, *38*(7), 2967–2985.

Mäkinen, H., Cano, J. M., & Merilä, J. (2006). Genetic relationships among marine and freshwater populations of the European three-spined stickleback (Gasterosteus aculeatus) revealed by microsatellites. *Molecular Ecology*, *15*(6), 1519-1534.

Mäkinen, H. S., & Merilä, J. (2008). Mitochondrial DNA phylogeography of the three-spined stickleback (Gasterosteus aculeatus) in Europe—evidence for multiple glacial refugia. *Molecular Phylogenetics and Evolution*, *46*(1), 167-182.

Nei, M. (1973). Analysis of gene diversity in subdivided populations. *Proceedings of the National Academy of Sciences USA*, *70*(12), 3321-3323.

Nei, M., & Li, W. H. (1979). Mathematical model for studying genetic variation in terms of restriction endonucleases. *Proceedings of the National Academy of Sciences*, *76*(10), 5269-5273.

Ota, R., Waddell, P. J., Hasegawa, M., Shimodaira, H., & Kishino, H. (2000). Appropriate likelihood ratio tests and marginal distributions for evolutionary tree models with constraints on parameters. *Molecular Biology and Evolution*, *17*(5), 798-803.

Parmesan, C. (2006). Ecological and Evolutionary Responses to Recent Climate Change [review-article]. *Annual Review of Ecology, Evolution, and Systematics*, *37*, 637-669.

Pickrell, J., & Pritchard, J. (2012). Inference of population splits and mixtures from genome-wide allele frequency data. *Nature Precedings*, 1-1.

Ralph, P. L., & Coop, G. (2015). The role of standing variation in geographic convergent adaptation. *The American Naturalist*, *186*(S1), S5-S23.

Ravinet, M., Yoshida, K., Shigenobu, S., Toyoda, A., Fujiyama, A., & Kitano, J. (2018). The genomic landscape at a late stage of stickleback speciation: High genomic divergence interspersed by small localized regions of introgression. *PLoS Genetics*, *14*(5), e1007358.

Razgour, O., Forester, B., Taggart, J. B., Bekaert, M., Juste, J., Ibáñez, C., Puechmaille, S. J., Novella-Fernandez, R., Alberdi, A., & Manel, S. (2019). Considering adaptive genetic

variation in climate change vulnerability assessment reduces species range loss projections. *Proceedings of the National Academy of Sciences USA*, *116*(21), 10418-10423.

R Core Team (2020). R: A language and environment for statistical computing. R Foundation for Statistical Computing, Vienna, Austria. https://www.R-project.org/

RStudio Team (2020). RStudio: Integrated Development Environment for R. RStudio, PBC, Boston, MA. http://www.rstudio.com/

Sanz, N., Araguas, R. M., Vidal, O., & Viñas, J. (2015). Glacial refuges for three-spined stickleback in the Iberian Peninsula: mitochondrial DNA phylogeography. *Freshwater Biology*, *60*(9), 1794-1809.

Schluter, D., & Conte, G. L. (2009). Genetics and ecological speciation. *Proceedings of the National Academy of Sciences USA*, *106*(Supplement 1), 9955-9962.

Schmitt, T. (2007). Molecular biogeography of Europe: Pleistocene cycles and postglacial trends. *Frontiers in Zoology*, *4*(1), 1-13.

Shanfelter, A. F., Archambeault, S. L., & White, M. A. (2019). Divergent Fine-Scale Recombination Landscapes between a Freshwater and Marine Population of Threespine Stickleback Fish. *Genome Biology and Evolution*, *11*(6), 1552-1572.

Stern, D. L., & Orgogozo, V. (2009). Is genetic evolution predictable? *Science*, *323*(5915), 746-751.

Stuart, Y. E., Veen, T., Weber, J. N., Hanson, D., Ravinet, M., Lohman, B. K., Thompson, C. J., Tasneem, T., Doggett, A., & Izen, R. (2017). Contrasting effects of environment and genetics generate a continuum of parallel evolution. *Nature Ecology & Evolution*, *1*(6), 1-7.

Terekhanova, N. V., Logacheva, M. D., Penin, A. A., Neretina, T. V., Barmintseva, A. E., Bazykin, G. A., Kondrashov, A. S., & Mugue, N. S. (2014). Fast evolution from precast bricks: genomics of young freshwater populations of threespine stickleback Gasterosteus aculeatus. *PLoS Genetics*, *10*(10), e1004696.

Thompson, K. A., Osmond, M. M., & Schluter, D. (2019). Parallel genetic evolution and speciation from standing variation. *Evolution Letters*, *3*(2), 129-141.

Tigano, A., & Friesen, V. L. (2016). Genomics of local adaptation with gene flow. *Molecular Ecology*, *25*(10), 2144-2164.

Vines, T.H., Dalziel, A.C., Albert, A.Y., Veen, T., Schulte, P.M. & Schluter, D. (2016). Cline coupling and uncoupling in a stickleback hybrid zone. *Evolution, 70*(5), 1023-1038.

Wang, S., Meyer, E., McKay, J. K., & Matz, M. V. (2012). 2b-RAD: a simple and flexible method for genome-wide genotyping. *Nature Methods*, *9*(8), 808-810.

Weir, B. S., & Cockerham, C. C. (1984). Estimating F-statistics for the analysis of population structure. *Evolution*, 1358-1370.

Willi, Y., Van Buskirk, J., & Hoffmann, A. A. (2006). Limits to the adaptive potential of small populations. *Annual Review of Ecology, Evolution, and Systematics*, *37*, 433-458.

Yoshida, K., Makino, T., Yamaguchi, K., Shigenobu, S., Hasebe, M., Kawata, M., Kume, M., Mori, S., Peichel, C. L., & Toyoda, A. (2014). Sex chromosome turnover contributes to genomic divergence between incipient stickleback species. *PLoS Genetics*, *10*(3), e1004223.

Yoshida, K., Miyagi, R., Mori, S., Takahashi, A., Makino, T., Toyoda, A., Fujiyama, A., & Kitano, J. (2016). Whole-genome sequencing reveals small genomic regions of introgression in an introduced crater lake population of threespine stickleback. *Ecology and Evolution*, *6*(7), 2190-2204.

Zanella, L. N., DeFaveri, J., Zanella, D., Merilä, J., Šanda, R., & Mrakovčić, M. (2015). Does predation drive morphological differentiation among Adriatic populations of the three-spined stickleback? *Biological Journal of the Linnean Society*, *115*(1), 219-240.

Zanella, L. N., Zanella, D., Mrakov, ić, M., Miletić, M., Mustafić, P., & Ćaleta, M. (2009). Occurrence of four-spined Gasterosteus aculeatus in an isolated Croatian river population. *Journal of Fish Biology*, *75*(8), 2052-2061.

Zecca, G., Labra, M., & Grassi, F. (2020). Untangling the Evolution of American Wild Grapes: Admixed Species and How to Find Them. *Frontiers in Plant Science*, *10*, 1814.

Zheng, X., Levine, D., Shen, J., Gogarten, S. M., Laurie, C., & Weir, B. S. (2012). A high-performance computing toolset for relatedness and principal component analysis of SNP data. *Bioinformatics*, *28*(24), 3326-3328.

DATA ACCESSIBILITY

Raw sequence data have been deposited to GenBank (BioProject PRJNA779581, Short Reads Archive SRR16935943-SRR16936116). Scripts and processed data are available at Zenodo data repository (doi: 10.5281/zenodo.5653575). The pipeline for TreeMix analyses are also available via GitHub (https://github.com/carolindahms/TreeMix), as well as scripts for demographic modelling (https://github.com/carolindahms/moments). All supplementary tables and figures cited in the main text have been uploaded as online Supporting Information.

AUTHOR CONTRIBUTIONS

J.M., P.M. and C.D. conceived the study, C.D. analysed the data with help and feedback from P.M., P.K. performed the linkage disequilibrium network analyses with linear mixed models. L.Z. and D.Z. provided Albanian and Greek samples, while A.C. was responsible for Italian *G. aculeatus* samples. C.D. wrote the first draft, and all authors contributed to subsequent versions of the manuscript.

TABLES AND FIGURES

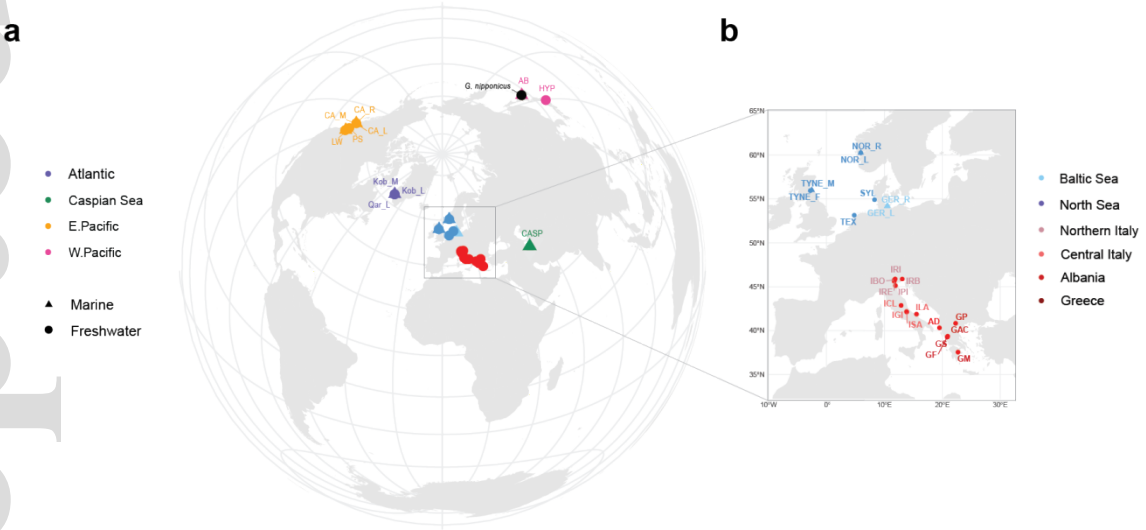

Figure 1 | Location of samples. a, World map showing the location of the *G. aculeatus* populations analysed and their respective ecotypes (circles – freshwater, triangles – marine). Sample location of *G. nipponicus* is shown in black. **b,** Location of European populations. Samples are coloured according to geographic region. In the European map, the Trans-Atlantic group is further split into North Sea (dark

blue) and Baltic Sea (light blue), while the Adriatic sampling consists of Greek (dark red), Albanian (red), North Italian (salmon) and Central Italian (orange red) populations.

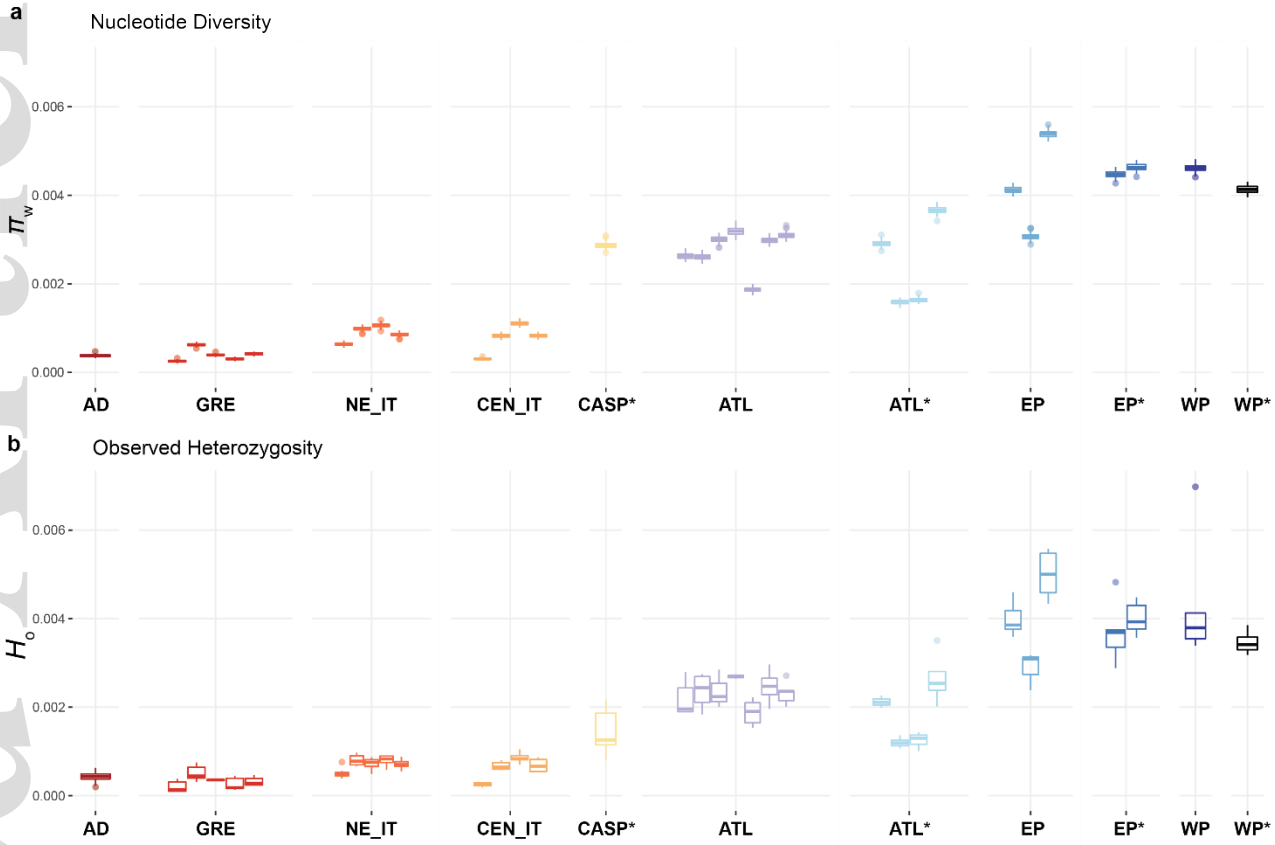

Figure 2 | Genetic diversity. a, Nucleotide diversity (π) calculated for each population from 100 site allele frequency spectra (SFS) bootstrap replicates and grouped into regions; marine populations are indicated by asterisks (*). **b,** Observed heterozygosity (H_o) averaged over each population, grouped into the same regions as above.

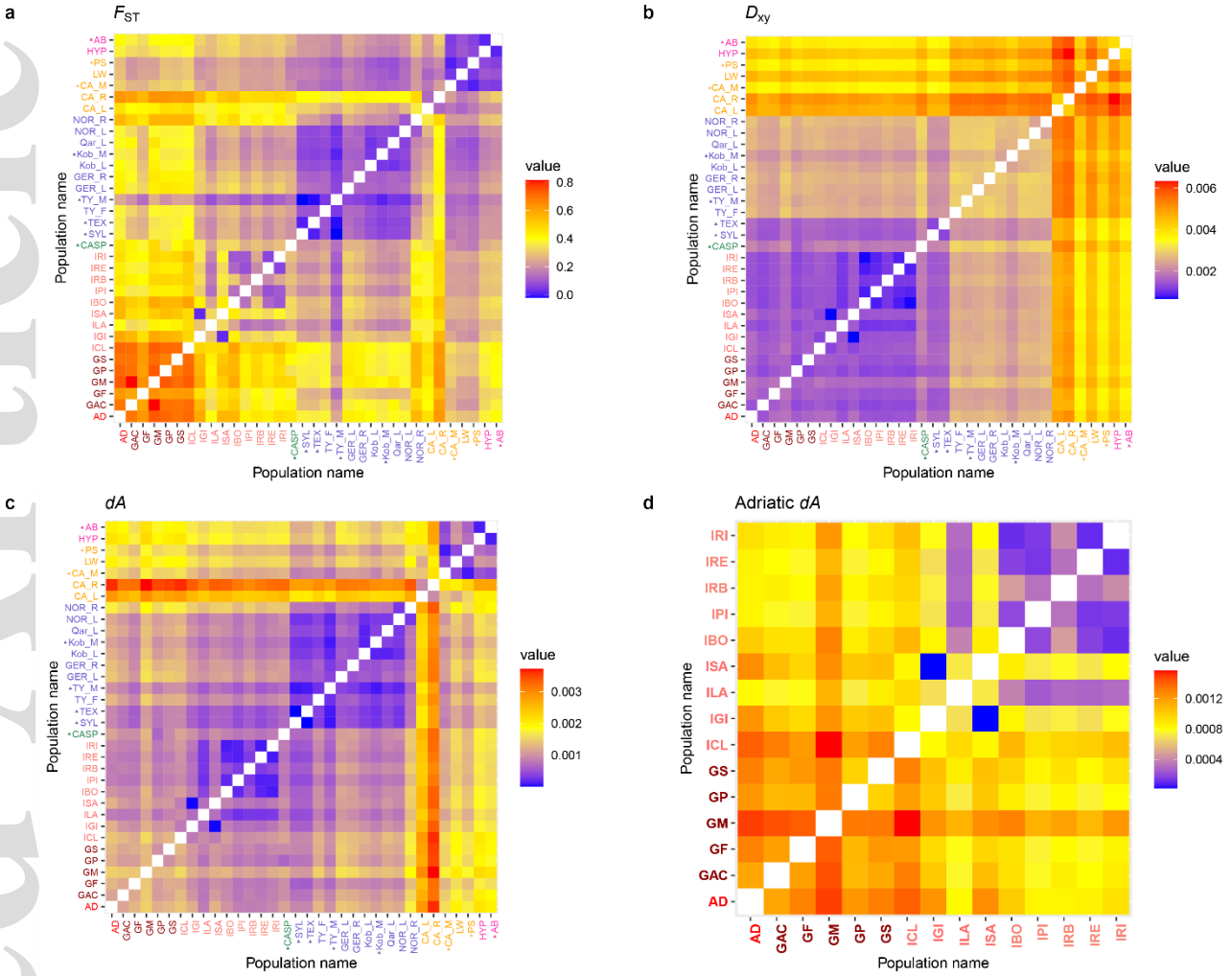

Figure 3 | Genetic differentiation. a, pairwise F_{ST} matrix. Populations are grouped and coloured according to geographic region: Adriatic Sea (red), Caspian Sea (green), Trans-Atlantic (blue), Eastern Pacific (orange), Western Pacific (pink) showing clusters of high differentiation in the Adriatic and low genetic differentiation in the Pacific and Trans-Atlantic. Marine ecotype is indicated by triangles. **b,** pairwise absolute divergence (D_{xy}) matrix grouping populations as above. Patterns of divergence broadly corresponded to three geographic regions, gradually decreasing from the Pacific to the Adriatic Sea. **c**, matrix representing pairwise 'net' divergence estimates (*dA*), obtained by correcting D_{xy} for ancestral diversity (average nucleotide differences among two populations before divergence). Clusters of low degree of divergence emerged in the Pacific, Trans-Atlantic and Adriatic-Italian populations. **d,** *dA* estimates for the Adriatic populations, showing clusters of low divergence in the Italian region and higher net divergence in Albanian and Greek populations, with the GM lineage standing out.

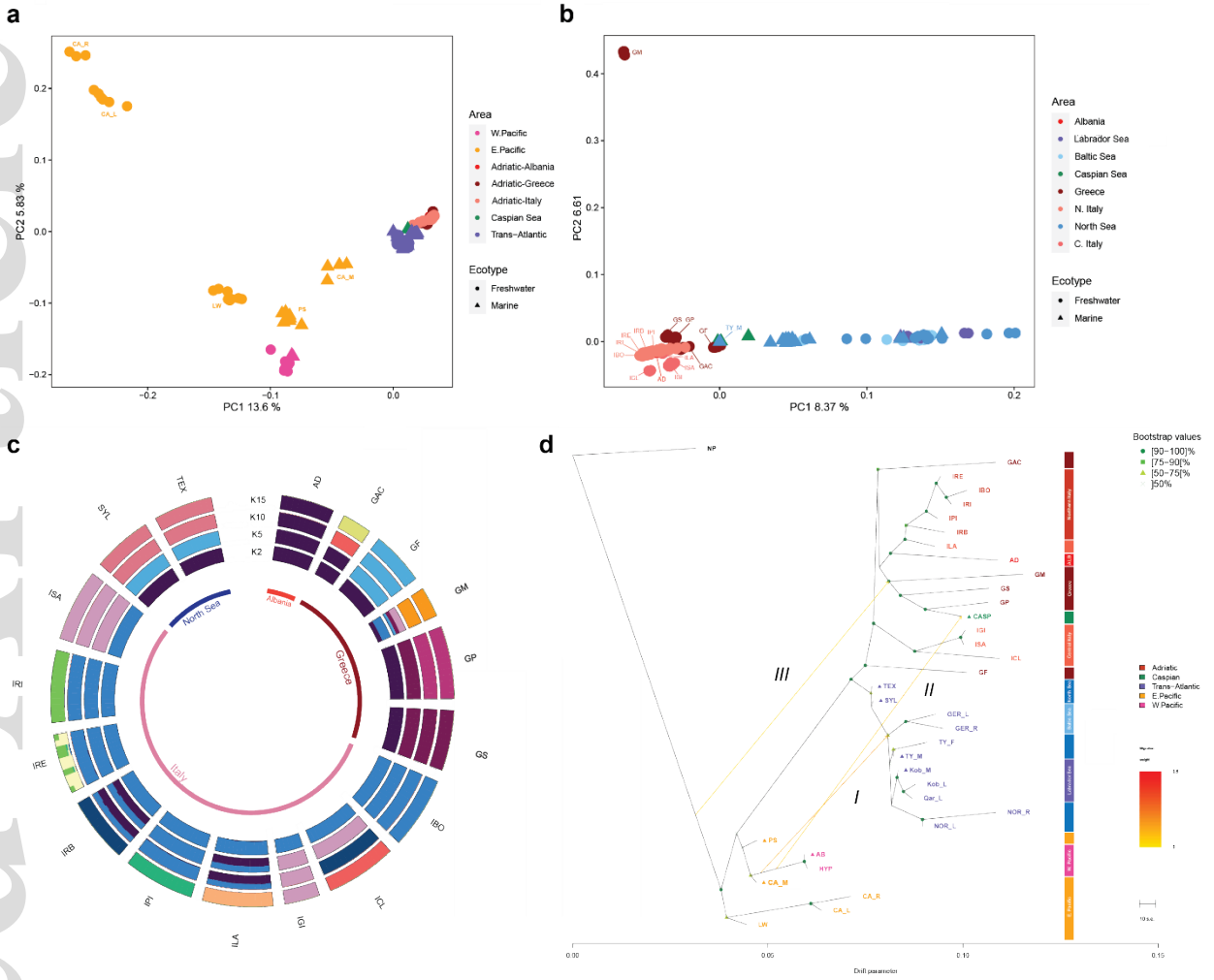

Figure 4 | Population structure. a, PCA representing geographic structure among the Pacific (orange and pink), Trans-Atlantic (blue), Caspian (green) and Adriatic Sea (different shades of red for each sub-region). **b,** PCA performed excluding the Pacific regions, showing further population structuring. The Trans-Atlantic is further split into Atlantic (purple), North Sea (dark blue) and Baltic Sea (light blue). PC1 axis explains within region variation among the Trans-Atlantic and separates Greek lineages from the rest of the Adriatic, with GF clustering close to the Caspian and North Sea and GM separating from everything else along PC2. **c, ADMIXTURE** results plotted for K = 2, K = 5, K = 10, K = 15. According to cross validation errors, 15 was the optimum number of clusters. The inner circle groups populations into respective regions: North Sea (marine) and three freshwater Adriatic sub-regions (Albania, Greece, Italy). **d, Maximum likelihood tree inferred by TreeMix.** Population names are coloured according to region: orange – Eastern Pacific, pink – Western Pacific, blue – Trans-Atlantic (divided into sub-regions North Sea (dark blue), Labrador Sea (purple blue), Baltic Sea (light blue)), red – Adriatic Sea (comprising of Albania (red), Greece (dark red), central Italy (orange red), northern Italy (salmon)), while *G. nipponicus* (in black)

is set as the outgroup. Marine populations are indicated by triangles. Bootstrap values represented in percentage from all (500) bootstrap replicates are shown for each node, with exceptions where tree topology from the consensus tree was changed by TreeMix. Three migration edges are numbered (I-III), with the direction of admixture indicated by arrows and coloured according to migration weight, i.e., the ancestry percentage received from the donor. Branch length indicates the degree of genetic drift from the last common ancestor, and the scale bar shows 10 × the average standard error of the sample covariance matrix. Residual and drift matrices are provided in Supplementary Figure S2.

Table 1 | Support for migration edges. Migration events inferred by TreeMix (Figure 4d) are numbered (I – III), indicating source (the set of species found in the subtree below the origin of the migration edge) and recipient (the set of species found in the subtree below the destination of the migration edge). For each migration edge, the number of independent runs (*N*) used to calculate mean values, the mean weight of the migration($\bar{w}$), the mean jackknife estimate of the weight ($\bar{w_j}$) and the jackknife estimate of the standard error ($\bar{SE_j}$) averaged over *N*, as well as the least significant p- value recovered from all runs are indicated.

Migration edge	Source	Recipient	w	$\bar{wj}$	$\bar{SEj}$	p-value	N
I	*AB, HYP*	*GER_L, GER_R, Kob_L, Kob_M, NOR_L, NOR_R, Qar_L, TY_F, TY_M*	0.12185	0.121865	0.009617	<0.0001	30
II	*AB, HYP*	*CASP*	0.057669	0.057643	0.011899	<0.0001	30
III	*AB, AD, CA_L, CA_M, CA_R, CASP, GAC, GER_L, GER_R, GF, GM, GP, GS, HYP, IBO, ICL, IGI, ILA, IPI, IRB, IRE, IRI, ISA, Kob_L, Kob_M, LW, NOR_L, NOR_R, PS, Qar_L, SYL, TEX, TY_F, TY_M*	*CASP, GM, GP, GS*	0.029969	0.029971	0.010037	0.001413	30

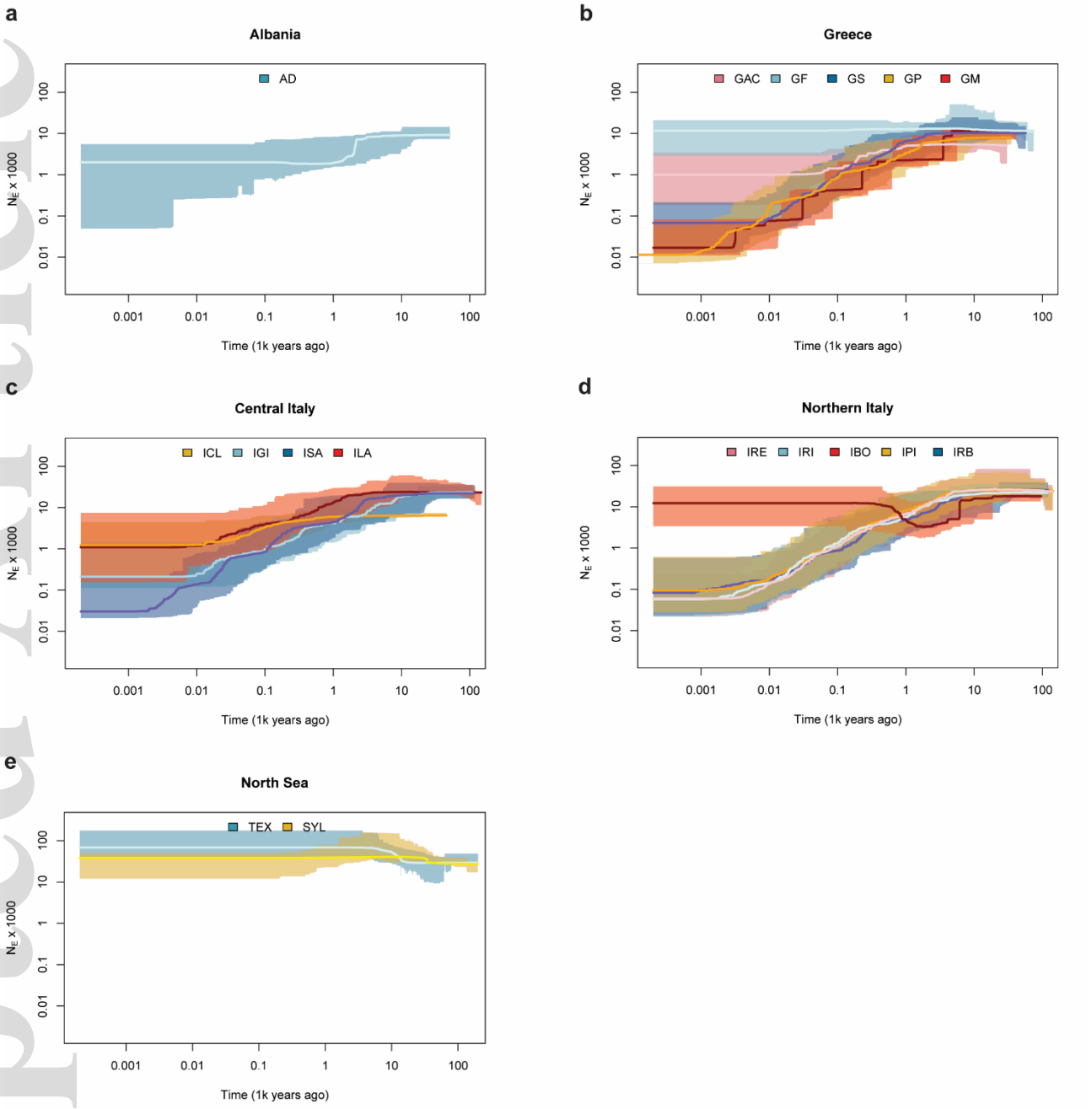

Figure 5 | Historical changes in N_e. Sizes of N_e over time obtained by Stairway plots in the Adriatic (**a**-**d**) and the North Sea (**e**). Lines represent medians, and polygons 95% confidence intervals. Plots were generated from folded one-dimensional site frequency spectra (SFS), including singletons assuming a generation time of 2 years and a mutation rate of 1×10^{-8} per site/year. Estimations with mutation rates of 7.1×10^{-9} and 3.7×10^{-8} can be found in Supplementary Figure S4.

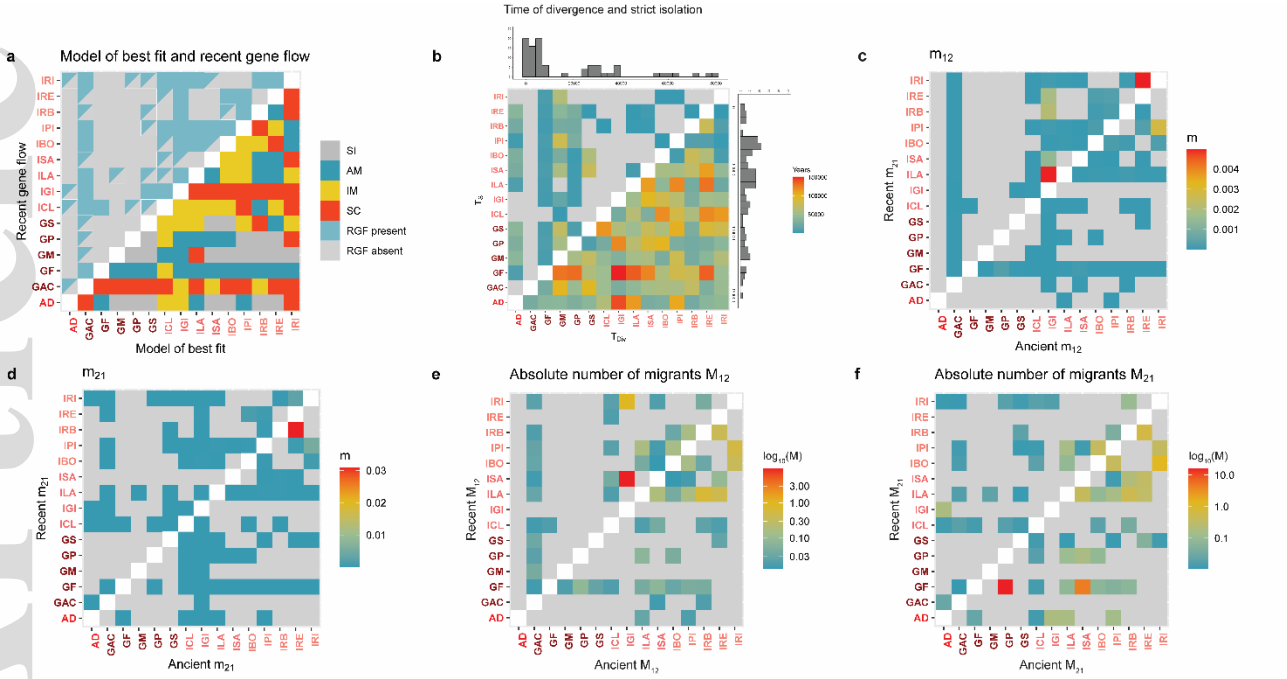

Figure 6 | Demographic history of Adriatic freshwater populations. a, Lower half of the matrix: model of best fit for each population pair suggested by demographic modelling with *moments* – SI (strict isolation), AM (ancient migration), IM (isolation with migration), SC (secondary contact) models. Upper half shows whether demographic models suggest recent gene flow (RGF) to be absent (grey) or present (light blue). Lack of gene flow is indicated by grey triangles (where models suggested less than 1 migrant per 100 generations). Populations are coloured according to geographic regions within the Adriatic Sea: Albania (red), Greece (dark red), central Italy (orange red) and northern Italy (salmon). **b,** Lower half: time of divergence (T_{DIV}) in years, calculated as the sum of all time parameter estimates for each population pair with histogram showing abnormal distribution in divergence estimates. Upper half: time of strict isolation (T_{SI}) in years among each population pair, calculated as the time without gene flow only for pairs with the SI and AM scenario. Population pairs with other models (IM, SC) are marked in grey, histogram shows distribution of isolation time estimates. **c,** Migration rate m_{12} occurring in recent times (populations with SC and IM models, upper matrix half) and during ancient migration scenarios (populations with AM and IM models, lower half). **d,** Migration rate m_{21} reported as in ***c***. Migration rates represent the proportion of the 1st population made up of migrants from the 2nd population (m_{12}) and *vice versa* (m_{21}). **e** and **f** show absolute number of migrants (M_{12} and M_{21}, respectively) on a $\log_{10}$ scale for all but exponential growth models, calculated from scaled migration rates and population sizes during time of migration.

Table 2 | Summary of outlier regions analysed. Shows original number of loci (N) for each region (ordered by chromosome and index of start position), as well as number of loci from cluster with

strongest asscociation with ecotype (N_{cl}), the nominal p-value (*p*) when including relatedness as a random effect and r^2, the effect size (cor^2). Mean PC-score results for each geographic area (*PC1*) are only shown for regions with p<0.05 with marine samples in brackets.

Region	N	N_{cl}	start	stop	*p*	r^2	$PC1_{EP}$	$PC1_{ATL}$	$PC1_{WP}$	PC_{AD}	$PC1_{CASP}$
Chr1_1	47	2	12324	12339	0.0542	0.041	-	-	-	-	-
Chr1_2	992	2	21492	21938	7.99E-17	0.543	0.833(0.018)	1(0.695)	0(0)	0.991	0
Chr4_1	142	35	12800	12878	3.01E-05	0.179	-	-	-	-	-
Chr4_2	22	2	15030	15036	0.128	0.0259	-	-	-	-	-
Chr4_3	167	5	19812	19915	3.89E-09	0.324	0.349(0.1)	0.846(0.583)	0(0)	0.921	0.001
Chr4_4	68	4	21815	21847	0.0608	0.0389	-	-	-	-	-
Chr4_5	60	11	23928	23982	0.000316	0.136	0.77(0.272)	0.16(0.099)	0.224(0.214)	0.041	0.097
Chr4_6	115	4	26030	26148	0.0172	0.06 21	0.726(0.109)	0.432(0.707)	0.052(0)	0.952	0.087
Chr8_1	34	5	8244	8258	0.0107	0.0709	0.36(0.047)	0.118(0.016)	0(0)	0.098	0
Chr9_1	45	7	8820	8860	0.0272	0.0536	0.519(0.33)	0.922(0.844)	0.312(0.591)	0.918	0.937
Chr9_2	30	4	9911	9935	0.0605	0.039	-	-	-	-	-
Chr11_1	520	7	5441	5853	1.87E-17	0.558	0.95(0.051)	0.656(0.037)	0.014(0.017)	0.065	0.021
Chr16_1	34	7	4785	4824	0.294	0.0123	-	-	-	-	-
Chr20_1	118	3	181	264	0.00127	0.111	0.891(0.031)	0.748(0.362)	0.545(0.303)	0.85	0.276
Chr20_2	104	5	8638	8916	0.00084	0.118	0.079(0.009)	0.418(0.054)	0.036(0)	0.034	0

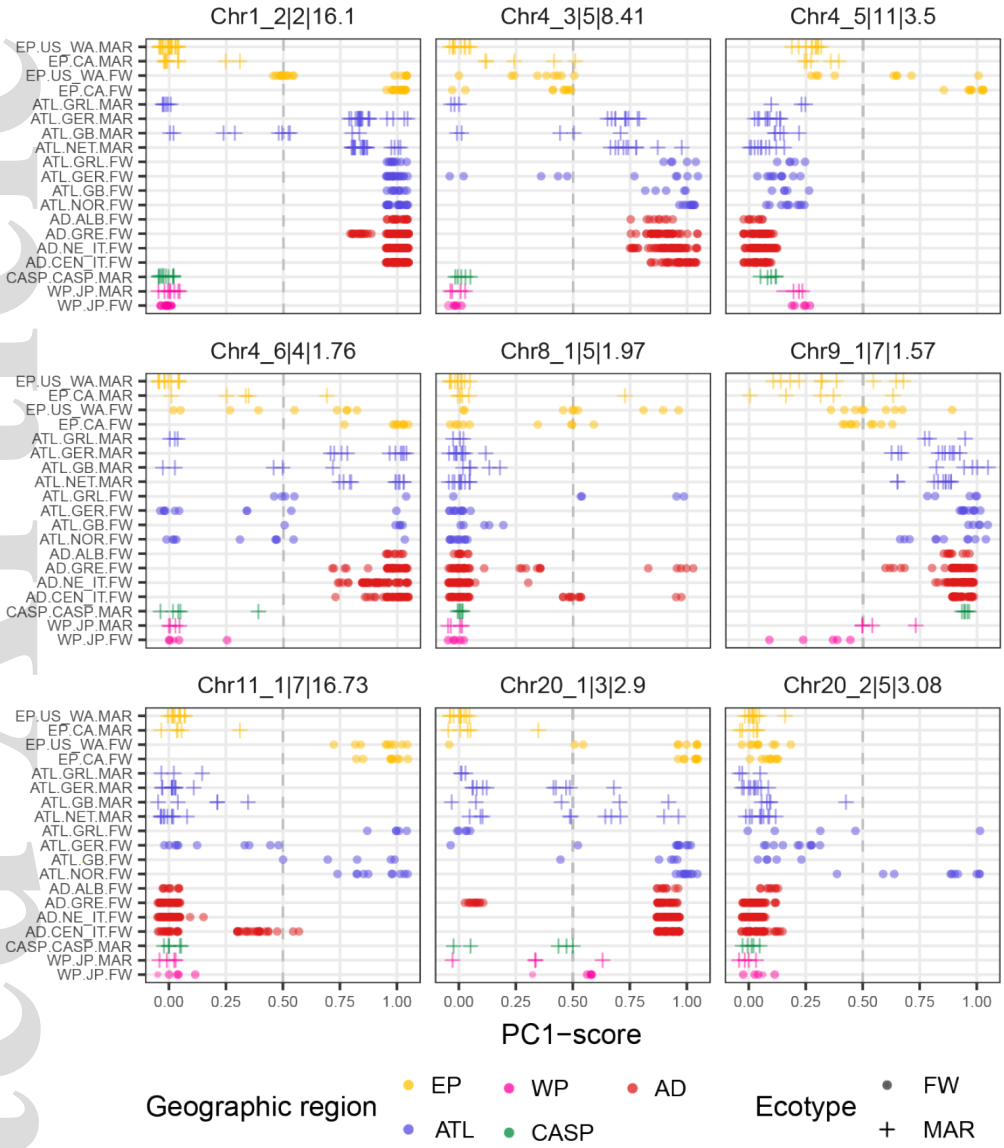

Figure 7 | Marine-freshwater PC1-score separation for significant outlier regions. Shows PC1-scores for the most significant nested sets of SNPs from LD-based single linkage clustering trees for genomic regions significantly associated with ecotype ($p<0.05$) in the Eastern Pacific and Atlantic Oceans. PC1-scores are scaled between [0,1] where individuals with freshwater adapted alleles are expected to cluster at PC1 ~1, and marine individuals at ~0. Figure titles are composed of region name, number of SNPs and -log10(P), separated by "|". Y-labels are composed of ocean (Eastern Pacific (EP), Atlantic (ATL), Western Pacific (WP), Caspian Sea (CASP) and Adriatic (AD)), location and ecotype separated by "." Colour indicates ocean and shape ecotype according to the legend. A small amount of noise has been added to the scores to improve visibility.

SUPPLEMENTARY FIGURE AND TABLE LEGENDS

Supplementary Table S1 | Sample Information. Information on species, region, location (for the Adriatic and Trans-Atlantic in the text also referred to as sub-regions), samples IDs, ecotype, coordinates and studies from which samples where re-acquired.

Supplementary Figure S1 | Admixture. Population structure inferred by ADMIXTURE for clusters K = 2-15. Analysis was performed on SNP data pruned for linkage disequilibrium. 15 was the optimum number of clusters, based on cross validation standard errors.

Supplementary Figure S2 | Residuals and drift estimates from Maximum likelihood tree. a, Pairwise residuals from the ML inferred by TreeMix (Figure 4d), with populations coloured according to region: orange – Eastern Pacific, pink – Western Pacific, blue – Trans-Atlantic (divided into sub-regions North Sea (dark blue), Labrador Sea (purple blue), Baltic Sea (light blue)), red – Adriatic Sea (comprising of Albania (red), Greece (dark red), central Italy (orange red), northern Italy (salmon)). Positive residuals suggest closer relationship between populations than as inferred by the tree (Figure 4d), while negative residuals indicate more distant relationship. **b,** Pairwise drift estimates from the ML tree (Figure 4d) calculated under Gaussian model, with populations coloured according to region as above.

Supplementary Figure S3 | Stairway plots excluding singletons. Sizes of N_e over time obtained by Stairway plots in the Adriatic and two marine North Sea populations (SYL and TEX). Lines represent medians, and polygons 95% confidence intervals. Plots were generated from folded one-dimensional site frequency spectra (SFS), excluding singletons, assuming a generation time of 2 years and a mutation rate of 1×10^{-8} per site/year.

Supplementary Figure S4 | Sizes of N_e over time. Historical changes in N_e were inferred by Stairway plots in the Adriatic and two marine North Sea populations (SYL and TEX). Lines represent medians, and polygons 95% confidence intervals. Plots were generated from folded one-dimensional site frequency spectra (SFS), including singletons assuming a generation time of 2 years and a mutation rate of 7.1×10^{-9} and 3.7×10^{-8} per site/year.

Supplementary Table S2 | Parameter estimates for best fitting models. From competing demographic models, the best fitting model was selected for each population pair, based on the Akaike Information Criterion ($\Delta AIC \geq 7$) where a likelihood ratio test was not appropriate. $\theta = 4N_{ANC}\mu$; n_1 and n_2 are current N_e sizes of population *i* and *j*, respectively. Other N_e estimates apply only to certain models: $n_{1b,}$ $n_{2b,}$ $n_{10,}$ n_{20} for Growth models (G), and $n_{1b,}$ n_{2b} for NeC models. N_e sizes are given in units relative to N_{ANC}. T_1 is time of split, and T_2 is time of secondary contact, which are given in units of $2N_{ANC}$ generations. Migration rates m_1 and m_2 represent migration from *j* to *i* and migration from *i* to *j*, respectively, and are given in units M_{ij} =

$2N_{ANC}m_{ij}$, where M_{ij} is the proportion of individuals in population *i* that is made up of migrants from population *j* at a given generation.

Supplementary Figure S5 | Graphical representations of demographic models tested. a, All models assume an ancestral population (N_{ANC}) splitting into two daughter populations (N_1 and N_2) at T_1. SI (strict isolation), IM (isolation with migration) models have only time of split (T_1) estimates with IM allowing for migration throughout (black arrows); while in the SC (secondary contact) model migration begins at time of secondary contact (T_2) and *vice versa* for the AM (ancient migration) model. **b,** NeC model modifications account for instantaneous population size changes in the daughter populations, estimating population sizes after T_1 (N_1, N_2) and T_2 (N_{1b}, N_{2b}). **c,** Growth models account for exponential growth during both T_1 and T_2 time periods. N_{10} and N_{20} represent daughter population sizes at time of split, N_1 and N_2 are population sizes at T_2, and N_{1b} and N_{2b} are final population sizes. Time occurs from top to bottom, with width of shapes representing changes in population size through time.

Supplementary Figure S6 | Residuals and SFS. Inferred and observed Site Frequency Spectra (SFS) and residuals of best fitting models for each Adriatic population pair computed with *moments v.1.1.0***.**

Supplementary Figure S7 | Single-linkage clustering trees based on LD. Linkage disequilibrium network analyses were performed separately for the 15 outlier regions analysed. Shown are the resulting hierarchical single-linkage clustering trees based on pairwise LD-values between loci, with clades and branches coloured by -log10(p) from the EMMAX analyses testing for correlation between PC1-scores (for each clade) and ecotype as binary trait [0,1]. Only the clade with the highest significance in the entire tree was used for downstream analysed (indicated by text). X-axis shows the weakest link (LD-value) among any of the loci in a given cluster.

Supplementary Table S3 | Summary of PC1 and cluster separation scores. Shows mean PC1 scores for freshwater ($PC1_{fw}$) and marine ($PC1_{mar}$) samples, respectively, separated by "/", and cluster separation scores (CSS; $PC1_{fw}$-$PC1_{mar}$) is shown in brackets (CSS=1 indicates that marine and freshwater samples are fixed for different SMLAs). Sample size (n) is for freshwater and marine samples, respectively separated by "/".